Volume 7 JUNE, 1936 Number 6

PHYSICS

A Journal of General and Applied Physics

A Study of Polarization Capacity and Electrode Condition*

IRVING WOLFF, *Research Division, RCA Manufacturing Company, Camden, N. J.*

(Received December 16, 1935)

In order to determine the relative effects of electrode condition, electrolyte and a number of physical parameters on electrolytic capacity, the capacity-frequency characteristics of a single cell, kept under carefully controlled conditions, were measured for a period of about six months. Some conclusions to be drawn are: (1) While the magnitude of the capacity can be varied over a wide range by change in electrode condition, the general shape of the capacity frequency characteristic is determined mostly by the concentration of the active ion in the electrolyte. (2) The capacity can be decreased greatly by exposing the electrodes to catalytic poisons such as H_2S and CO and can be subsequently increased by exposure to either electrolytic oxygen or hydrogen. These effects can be alternated. (3) The capacity is less subject to variations at the higher than the lower frequencies.

THE investigations, which are described in this article, are a continuation of some experiments which have already been reported by the same author.[1] In the first set of experiments the capacity of either platinum or gold electrodes in sulphuric acid was studied by means of alternating currents whose frequencies varied from a few hundred to 200,000 per second. The relation between capacity and frequency could be represented over a very wide range by a law of the form $C = \text{const} \times f^{-m}$ where C is polarization capacity, f is frequency and m is a constant of the order of magnitude 0.3. At the higher frequencies there were indications of breaking away from this law, the coefficient changing to the neighborhood of 0.5.

The magnitude of the polarization capacity C is defined in the way it has been used in the previous article and in accordance with the usage adopted by Warburg[2] and Kruger[3] and should not be confused with the measured capacity. A very good discussion of the meaning of different measurements of C is given in the first page of the article by Murdock and Zimmerman which is appearing in this same issue. In the following presentation, since the phase angle was not measured the values of capacity which are given are what Murdock and Zimmerman have called C_s which is the directly measured equivalent series electrical capacity. In view of the fact that the main conclusions which are drawn in this discussion can be deduced from comparative measurements, the capacities have been plotted as measured for the complete cell and have not been converted to capacity per unit area for a single electrode as in the preceding article. The conversion may be made by multiplying the values which are given by 16 which is twice the reciprocal of the area of one electrode.

Previous experimenters have been greatly troubled by the variations and apparently mysterious changes in the values of the polarization capacity.

It was one of the main objects of this set of experiments to try to control this shift in the capacity, or at least, if this was not possible, to try to determine the rate and cause of the change. In order to do this, all physical and

* The experimental part of this work was completed at the Physical Laboratory of Cornell University during 1924 and was made possible by a grant from The Heckscher Research Council of Cornell University.

[1] Wolff, Phys. Rev. **27**, 755 (1926).

[2] Warburg, Ann. d. Physik **303**, 492 (1899); **311**, 125 (1901).

[3] Kruger, Physik. Zeits. **45**, 1 (1904).

chemical conditions were kept as uniform as possible and then changed one by one, allowing plenty of time between each change for a new equilibrium to be reached. Whenever possible, a return was made to the original conditions. Instead of using a number of cells with electrodes which could vary in unknown ways, a single cell was carried through a constantly known set of conditions for a period of about six months. The complete history of the cell during these six months is given on a later page. Whenever any important change had been made or after the cell had been in any condition for an appreciable period of time, a complete measurement of its electrical capacity was made at a sufficient number of frequencies between a few hundred and 200,000 cycles to allow the determination of the polarization capacity.

Apparatus

The apparatus employed to make the capacity measurements was similar to that which had been used by the author in the preceding experiments.[1] A number of refinements were made, however, to increase the accuracy. Separate bridges were used to make the measurements in the audible and super-audible ranges, shielding was improved, and correction was made when necessary for inductance in the resistance boxes.

The polarization capacity depends on temperature.[4] There was also the possibility that the drift would vary with the temperature. The cell was therefore kept at zero degrees C in an ice-filled Dewar flask, at 35°C by means of a thermostat, or for longer periods of time at close to 0°C in an ice box.

The cell used in the previous experiments had the electrodes sealed into glass by means of De Khotinsky cement. In accordance with the plan to keep all physical and chemical factors as much under control as possible, it was decided to eliminate the De Khotinsky and seal the platinum electrodes directly into glass. The leads from the electrodes were also of platinum and had been soldered to the electrodes by means of gold solder. The cell shown in Fig. 1 was used for all measurements. Any polution of the electrolyte in this cell was limited to that caused by the glass of test tube and other cell parts or

[4] Zimmerman, Phys. Rev. **35**, 543 (1930).

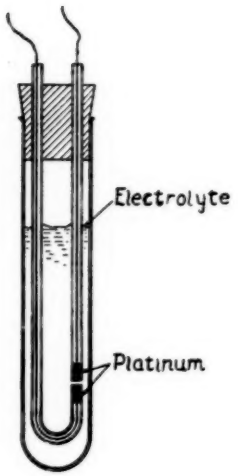

Fig. 1. Cell details.

that caused by vapors given off by the rubber stopper.

The electrodes had been treated as follows before use. They had been heated to a temperature of at least 1000°C for the gold soldering operation. In sealing into the glass they had been heated again, but not to such a high temperature. The end of the electrode in its sheath of glass had afterward been ground down plane and perpendicular to the axis of the cylinder on a grindstone. Succeeding this, it had been polished with emery cloth and jeweler's rouge. Directly afterwards it was washed in distilled water where it remained until used.

When not in the bridge circuit or in use, the cell was kept at all times on short circuit. This precaution was necessary in order to keep conditions at the electrodes uniform.

Experimental Results

Experiments by various observers have shown that the capacity is affected by the following factors:

1. Material and condition of the electrode
2. Electrolyte substance
3. Concentration
4. Temperature
5. Frequency

In these experiments the material making up the electrode was kept constant (bulk platinum) and precautions were taken as described above, to keep its surface from being influenced by

TABLE I. *Pertinent data on the history of the polarization cell.*

DAY	CONDITION AND TREATMENT	CAPACITY (μf) AT 660 CYCLES PER SECOND	CURVE NO.	FIGURE NO.
1	Put in 2 normal H_2SO_4 at 23°C	1.3		2
	Cell put in ice 0°C			2
1–2	At 0°C			2
2	C.F.R. 0°C	0.75	1	3
2–17	0°C			2
17–36	In ice box			2
36	Test tube broke new 2 *N* H_2SO_4 added			2
37	C.F.R. 0°C	.65	2	3
	Temp. raised to 35°C			2
38	C.F.R. 35°C	.87	3	3
38–42	Temp. at 35°C			2
42	Temp. to 0°C			2
43	Temp. to 35°C then return to 0°C			2
44	0.2 Normal H_2SO_4 at 0°C replaces 2 *N* H_2SO_4			2
	Return to 2 *N* H_2SO_4 at 0°C			2
	Replace with 0.2 *N* H_2SO_4 at 0°C			2
	C.F.R. 0.2 *N* H_2SO_4 at 0°C	.35	4	4
44–48				2
48	Temp. raised to 35°C			2
	C.F.R. 35°C	.49	5	4
	Temp. reduced to 0°C			2
48–49	Electrode exposed to H_2S during night			2
49	C.F.R. 0°C	.27	6	4
49–63	At 0°C and room temp.			
63–79	Room temp.			
79	Temp. at 0°C			2
	C.F.R. 0°C	.20	7	4
79–82	Room temp.			
82	Temp. 0°C			2
	Temp. increased to 35°C			2
82–83	35°C			2
30	C.F.R. 35°C	.28	8	4
84	0.2 *N* H_2SO_4 replaced by 2 *N* H_2SO_4 0°C			2
	C.F.R. 0°C	.34	9	3
85	Temp. increased to 35°C			2
	C.F.R. 30°C	.51	10	3
85–86	35°C			2
86	Electrode exposed to electrolytic hydrogen			2
87	C.F.R. 0°C	.47	11	3
87–89	Additional exposure to hydrogen			2
89	C.F.R. 0°C	1.8	12	3
89–90	Additional exposure to hydrogen			2
90	C.F.R. 0°C	1.6	13	3
90–91	Electrode exposed to electrolytic oxygen			2
91	C.F.R. 0°C	4.8	14	3
91–92	Additional exposure to hydrogen			2
92	A.F.R. 0°C	4.2	14	3
92–105	In ice box			2
105	C.F.R. 0°C	2.7	15	3
106	2 *N* H_2SO_4 replaced by 0.2 *N*			2
	C.F.R. 0°C	1.6	16	4
106–107	Electrode exposed to H_2S			2
107	0°C			2
107–108	Exposed to H_2S			2
108	C.F.R. 0°C	0.58	17	4
108–109	Electrode exposed to electrolytic oxygen			2
109	0°C	2.7		2
	0.2 *N* H_2SO_4 replaced by 0.02 *N* H_2SO_4			
109–112	0°C			
112	A.F.R. 0°C	1.4	18	5
114	A.F.R. 0°C	1.1	18a	5
115	0.02 *N* H_2SO_4 replaced by 0.001 *N* H_2SO_4			
	A.F.R. 0°C	0.60	19	5
	Temp. raised to 45°C	.84		
118	A.F.R. 45°C	.77	20	5
	Temp. raised to 73°C	.96		
	Reduced to 41°C	.79		
120	0.001 *N* H_2SO_4 replaced by 0.2 *N* H_2SO_4 0°C	1.7		
	0.2 *N* H_2SO_4 replaced by *N* HCl 0°C	2.6		
121	*N* HCl replaced by 0.1 *N* HCl 0°C	1.7		
	C.F.R. 0°C	1.6	21	6
122	0.1 *N* HCl replaced by *N* HCl 0°C			
	C.F.R. 0°C	2.8	22	6
125	*N* HCl replaced by 0.01 *N* HCl 0°C			
	A.F.R. 0.01 *N* HCl 0°C	1.0	23	6
126	A.F.R. 0.01 *N* HCl 43°C	1.4	24	6
	A.F.R. 0.001 *N* HCl 30°C	0.91	25	6
	0.001 *N* HCl replaced by 0.2 *N* H_2SO_4 24°C	2.6		
126–127	Electrode exposed to CO overnight			
127	0.2 *N* H_2SO_4 22°C	1.5		
	Electrode exposed to CO			
	0.2 *N* H_2SO_4 21°C	1.4		
128	C.F.R. 20°C	1.1	26	4
128–131	Electrode exposed to CO			
131	0.2 *N* H_2SO_4 22°C	0.92		
	Electrode exposed to CO			
	0.2 *N* H_2SO_4 23°C	.81		
131–132	Electrode exposed to CO			
132	C.F.R. 25°C	.70	27	4
134	C.F.R. 0°C	.58	28	4 and 7
134–135	0°C	.57		
135	0.2 *N* H_2SO_4 replaced by 0.02 *N* H_2SO_4			
	A.F.R. 0°C	.31	29	7
	0.02 *N* H_2SO_4 replaced by 0.001 *N* H_2SO_4			
	A.F.R. 0°C	.15	30	7
	0.001 *N* H_2SO_4 replaced by 6 *N* H_2SO_4			
	C.F.R. 0°C	.99	31	7
138	3 *N* H_2SO_4 replaced by 20 *N* H_2SO_4			
	C.F.R. 0°C	1.1	32	7
139	20 *N* H_2SO_4 replaced by 2 *N* H_2SO_4			
	C.F.R. 0°C	1.1	33	7 and 1
140	0°C	1.1		
	Electrode exposed to electrolytic hydrogen			
	2 *N* H_2SO_4 0°C	2.7		
141	C.F.R. 0°C	1.9	34	3
142	0°C	1.8		

other substances than the electrolyte or known agents. Concentrations varied from 20 normal to 0.001 normal. Temperature was varied from 0 to 70°C, but mostly from 0 to 35°C, and the measurements were made at frequencies from 200 to 200,000 per second. The electrode condition was purposely changed, in addition to whatever incidental change was caused by the change in concentration and temperature, by exposure to electrolytic oxygen and hydrogen and by contact with some of the catalytic poisons, namely, hydrogen sulphide and carbon monoxide.

The complete history of the cell has been given in Table I for reference. The first column records the day measured from the time of first immersion in the electrolyte. The second column describes the condition of the cell, tests which were made on it, or treatment to which it was subjected. A.F.R. indicates capacity-frequency run from 200 to 6000 cycles, C.F.R. from 400 to 200,000 cycles. The third column gives the capacity at 660 cycles per sec. at the time when frequency runs were taken. This is to be used in conjunction with Figs. 3 and 4 where capacity-frequency characteristics have been plotted in groups on log-log paper in order to show the comparative shapes of the curves without reference to the absolute values which can be obtained from the table. The last two columns of Table I refer to the curves and figures where the data referred to in column 2 may be found.

Fig. 2 shows graphically the changes which took place in the capacity of the cell at 660 cycles per sec. for the first 109 days of immersion in electrolyte.

The experimental results will now be analyzed.

1. Effect of initial immersion in electrolyte on cell capacity

When the cell is first placed in the electrolyte the capacity decreases very rapidly for a time. Fig. 2 shows the rate at which this occurred for the cell treated as described. The initial test was made at room temperature so that immersion in the electrolyte would be the only disturbing factor. This decrease in capacity is in accord with results obtained by other observers. After a day in the acid the cell was maintained at 0°C so that constant conditions would obtain. After one month's immersion very little additional variation took place until some other variables were changed.

2. Change of capacity with temperature

It is well known that the capacity is a function of temperature. The extent to which the temperature coefficient depends on the frequency was studied from 400–200,000 cycles per sec. and from 0–35°C for 2 normal and 0.2 normal H_2SO_4 under various conditions (curves 2 and 3, also 9 and 10, Fig. 3, curves 4 and 5, also 7 and 8, Fig. 4). Within the limit of error of the measurements the temperature coefficients are independent of the frequency and concentration between the limits set forth above and are close to 0.01 per °C in agreement with Zimmerman.[4] In certain cases it was necessary to condition the electrodes by running over the temperature range several times in order to obtain reproducible results while at other times no such conditioning seemed

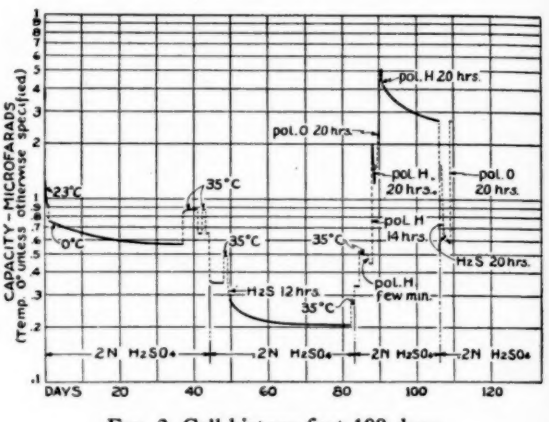

FIG. 2. Cell history first 109 days.

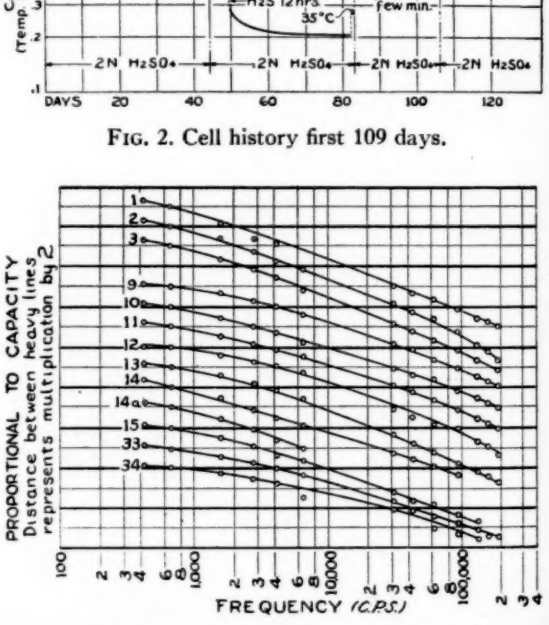

FIG. 3. Capacity-frequency data 2 N H_2SO_4.

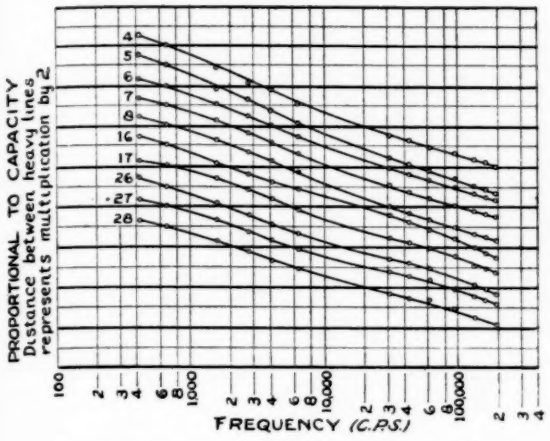

FIG. 4. Capacity-frequency data 0.2 N H_2SO_4.

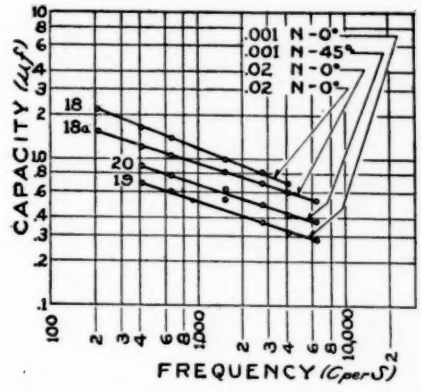

FIG. 5. Capacity-frequency data various concentrations H_2SO_4.

necessary. The temperature coefficient was also measured for 0.001 N H_2SO_4 from 0 to 45°C and 400–6000 cycles. In this range it was close to 0.008 per °C, little change being noticed as the frequency was varied. (See curves 19–20, Fig. 5.) The coefficient was nearly the same for 0.01 N HCl in the range from 200–6000 cycles and 0–43°C.

3. Effect of concentration on capacity

All the frequency runs which were taken with 2 N H_2SO_4 are plotted on Fig. 3 in order, those taken with 0.2 N on Fig. 4 also in order. These curves were obtained under a wide variety of electrode conditions as will be described in the next section and with a capacity at 660 cycles which varied from a minimum of approximately 0.2 μf to a maximum of 5 μf, a change of 25 times. The maintenance of the characteristic difference in shape between the sets of curves taken with 2 N and 0.2 N H_2SO_4 is very striking. In general the capacity decreases with the concentration, the percentage decrease being greater at the lower frequencies. The most notable difference lies in the slope m of the capacity-frequency curves. For 2 N this slope increases as the frequency rises whereas for 0.2 N it is almost constant over the range from 400 to 200,000 cycles. Another characteristic which is apparent both for 2 N and 0.2 N is the decrease in slope with time of immersion in the electrolyte. Whether this is connected with the rather varied treatment to which the electrodes were subjected or is generally true is not known. This change in slope is less at the higher frequencies and also for the lower concentrations.

On Figs. 5 and 7 capacity-frequency characteristics for some higher and lower concentrations are shown. For concentration 0.02 N and below, capacity was only measured up to 6000 cycles as the high electrolyte resistance of the cell made the measurements at higher frequencies uncertain.

Fig. 6 shows similar measurements for HCl ranging from 0.001 N to 1 N. Qualitatively the curves are similar in their characteristics to the corresponding curves for H_2SO_4.

4. Electrode condition

That the condition of the electrode affects the capacity and that it is difficult to maintain the electrode condition constant has often been observed. It is a change in electrode condition which presumably causes the decrease in capacity which takes place when the platinum is first immersed in the electrolyte. The increase in capacity after exposure of the surface to electrolytic hydrogen and oxygen has often been noticed.

If the capacity is so dependent on electrode surface condition it seemed that chemicals which have a large effect on reactions which depend on surface catalysis should change the capacity in magnitude and possibly in frequency dependence.

If we refer to Table I and Fig. 2 it will be noted that the cell after having been subjected to temperature variations from 0 to 35° and exposed to 2 N and 0.2 N H_2SO_4 for 48 days was placed for about 15 hours in distilled water

through which H_2S was bubbled. During the 4 days preceding this time, while the electrode had been in 0.2 N H_2SO_4 and had its temperature varied, the capacity had always returned to within a few percent of the original value when the same conditions of frequency and temperature were repeated.

After removal from H_2S exposure, the electrode was washed in distilled water and placed in the same 0.2 N H_2SO_4 at 0°C from which it had been removed the preceding day. The capacity had been reduced about 20 percent at 660 cycles. This decrease continued for a number of days. The curve of decrease is shown in Fig. 2 and indicated that a fairly stable condition was reached after 30 days. A frequency run indicated that the slope of the curve was less, i.e., the relative change in capacity was greater at the lower frequencies. This is shown in curves 5 and 6, Fig. 4, and in curves 3 and 9, Fig. 3. Curves 6, 7, 8, Figs. 4 and 9, 10, Fig. 3 show the effects of changing temperature and concentration on the treated electrodes. The relative changes in capacity seem to be about the same as previously. The characteristic shapes of the 2 N and 0.2 N concentration curves are also maintained.

Although the effect of exposing the electrode to hydrogen and oxygen was well known, it was considered worth while to spend a little time studying this effect in order to show how much the electrode capacity could be varied either up or down at will and in order to find out whether the shape of the frequency-capacity curves was still determined mainly by the concentration of solution, rather than by the electrode condition. A third electrode was accordingly added and made the positive pole of a decomposition cell, while the two regular electrodes tied together were made negative.

After several successive H treatments the capacity had been increased to about 5 times the value it had before this treatment was begun, and to a value a little greater than the initial value assumed when the cell was placed in sulphuric acid solution.

Capacity-frequency curves taken between H treatments showed essentially the same characteristics as had been shown in previous curves taken with 2 N H_2SO_4. The results of this treatment are shown in Fig. 2 and curves 10, 11, 12, 13 of Fig. 3. It will be noticed that the capacity increased more after each treatment at the low than the high frequency end, indicating again the greater relative constancy of the capacity at the higher frequencies.

The electrodes were next exposed to electrolytic oxygen by making them the positive pole of the cell with the third electrode. As is shown in Fig. 2 the capacity was increased again, this time to about three times its last preceding value. The capacity was now about 10 times what it was before H treatment. The capacity-frequency curve is shown in Fig. 3, curve 15. The characteristic shape of the 2 N H_2SO_4 curve is somewhat modified. Unfortunately the data were not plotted immediately after this experiment had been made and the apparatus was dismantled before the frequency curve after exposure to oxygen could be repeated so that no check on this was obtained.

After an additional H treatment and stabilization for 13 days, which resulted in a decrease of capacity of 30 percent at 660 cycles, the usual characteristic was obtained as is shown in curve 15, Fig. 3.

Replacement of the 2 N by 0.2 N H_2SO_4 showed the characteristic effects which had been noted in other cases for this change (see Fig. 2 and curve 16, Fig. 4). The interchange of 2 N and 0.2 N H_2SO_4 had now been carried out for unconditioned electrodes, those treated with H_2S, and after exposure to oxygen and hydrogen. In spite of the large change in capacity caused by electrode condition the proportionate change in going from the one concentration to the other

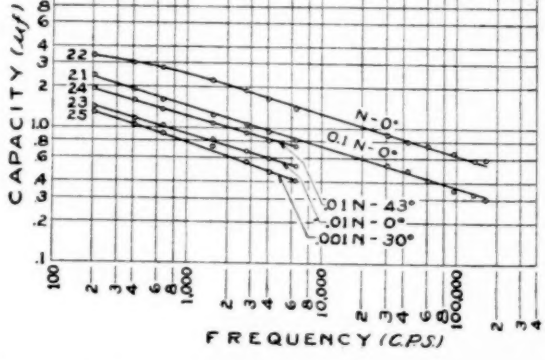

FIG. 6. Capacity-frequency data various concentrations HCl.

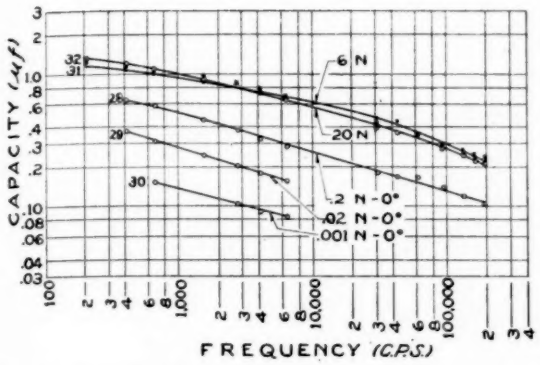

FIG. 7. Capacity-frequency data various concentrations H_2SO_4 (crosses indicate data for 2 N H_2SO_4 curve 33).

was the same within the limit of error of the measurements in all three cases.

In order to determine whether the capacity could be reduced again by H_2S treatment, the electrodes were exposed to H_2S in the same manner as was described previously. After 2 days exposure the capacity at 660 cycles had been reduced to 1/3 its preceding value and was showing indications of stabilizing at a somewhat lower figure. This is shown in Fig. 2 and the capacity-frequency curve is given in Fig. 4, curve 17. Under the influence of exposure to oxygen the capacity was raised again.

After a series of tests in which various lower concentrations of H_2SO_4 were tried, which have been described in the last section, and a series of tests in which HCl was substituted for H_2SO_4 which will be described in the next section, H_2S having been successful in reducing the capacity, another catalytic poison in the form of CO gas was tried. After successive exposure to carbon monoxide gas for a period of 5 days the capacity had been reduced to 1/4 its preceding value (see Table I, days 126–134). The capacity-frequency characteristic was changed very little—Fig. 4, curves 26, 27, 28.

5. Electrolyte

In order to see whether the capacity was determined mostly by the H ion, HCl was substituted for H_2SO_4 in a series of tests. These data are recorded in Table I days 120 to 126 and in Fig. 6, curves 21 to 25. The shape and slope of the capacity-frequency curves for corresponding concentrations of HCl and H_2SO_4 are the same within the limit of error of the measurements.

EXPERIMENTAL CONCLUSIONS

1. Treatment of electrodes by H_2S, CO, H and O

By means of exposure to H_2S and CO, substances of the class of catalytic poisons, it was found possible to reduce the capacity of the cell at will to a certain lower limit. This treatment did not hinder the increase of capacity by means of H and O polarization which had already been observed by other experimenters. The two types of treatment could be alternated to run the capacity up and down without apparent effect on each other. The reduction in capacity treatment is the slower to apply, successive treatments still causing a decrease in capacity after a few days exposure. It is interesting that the capacity stabilizes at a lower value in both cases. The direction of stabilization is in the direction of capacity change for the H_2S and CO treatment while it is opposite to the change which took place for O and H treatment.

2. Concentration of electrolyte

The capacity rises as the concentration is raised. For the lower concentrations (up to 0.1 N), the proportionate rise over the frequency range studied is almost the same at all frequencies. At the higher concentrations the rise in capacity no longer takes place, 2 N, 6 N and 20 N H_2SO_4, showing nearly the same capacity at all frequencies. Between 0.2 N and 2 N, the same proportionate change does not take place at all frequencies, the proportionate change being much smaller at the low end. The characteristic change of capacity as the concentration is changed takes place in nearly the same ratio for all conditions of the electrodes and at the two temperatures studied (0°C and 35°C). Over any small frequency region, the capacity can of course be expressed as a power function of the frequency $C_s = \text{const.}\, f^{-m}$. The exponent m is determined graphically by the slope of the curve at any point, when both C and f are plotted on logarithmic scales.

For the electrodes used, it was in the neighborhood of 0.3 for concentrations less than 0.2 N at all frequencies, the curve being remarkably close to a straight line over the range from 200–200,000 cycles. At the higher concentrations, the curve using the logarithmic scale has the slope of 0.3 from about 6000–50,000 cycles.

At the higher frequencies, it is represented by a larger number, at the lower frequencies by a smaller. Experiments made substituting HCl for H_2SO_4 show the same result, indicating that the effect is probably due to the H ion.

In this series of experiments, it was very clear that the shape of the capacity-frequency curve was determined more by the concentration than by the electrode condition, temperature, or any other single factor.

The shape of the curve was not found, however, to be entirely independent of these other factors. In general, when the capacity was changed, because of either temperature change or electrode condition change, there was a tendency to make the proportionate change less at the high frequencies than at the low, leading to steeper curves or greater values of the exponent m when some change was made which raised the capacity. This is in accord with the old experiments of Wien, who found a much greater proportionate change in capacity as the frequency was changed for platinized than for unplatinized electrodes.

3. Temperature coefficient

The capacity rises as the temperature rises. For the electrodes used the temperature coefficient, defined as $\Delta C_s/\Delta T \times C_s$, is almost 0.01 for 0.2 N and 2 N concentrations, in accord with Zimmerman's results at the lower frequencies. For 0.01 N and 0.001 N concentration the temperature coefficient is slightly lower. Within the limit of error of the experiment the temperature coefficient was found to be independent of the electrode condition. This in conjunction with the preceding sentence would indicate that it is an effect connected with the electrolyte.

In conclusion the author would like to express his appreciation to Professor C. C. Murdock of Cornell University for many helpful discussions and to Professors Murdock and Ernest Merritt for obtaining the equipment which made it possible to carry on this work.

Polarization Impedance at Low Frequencies

C. C. MURDOCK AND E. E. ZIMMERMAN, *Physical Laboratory, Cornell University*

(Received December 23, 1935)

The polarization capacity of a Pt-H_2SO_4-Pt electrolytic cell of concentration 0.25 N has been studied using alternating currents ranging in frequency from 0.05 to 3500 cycles per second and using aperiodic currents whose time constants range from 0.15 to 1.5 seconds. The empirical law, $C=13.6f^{-m}$, is found to hold throughout the frequency range with $m=0.11$. The angle ψ by which the current fails of quadrature with the polarization is constant within the accuracy of measurement and is in agreement with the Fricke relation, $\psi=\pi m/2$. The capacity as measured by aperiodic currents is found to increase slightly with the time constant. It is shown by a Fourier series expansion that if the alternating current results are correct, the aperiodic decay current is approximately exponential during the early part of the decay and that the measured polarization capacity is approximately proportional to the mth power of the time constant. The experimental data are in agreement with this conclusion.

THE variation of the polarization impedance of electrolytic cells with the frequency of the current has been the subject of much research since Kohlrausch in 1871 first made use of alternating currents to study polarization. The experimental results are usually expressed in terms of a polarization capacity, C, and the angle, ψ, which measures the amount by which the alternating current fails of being in quadrature with the electromotive force of polarization. Within the range of frequencies generally used it is found that ψ is independent of the frequency and that C varies inversely as a power of the frequency.

$$C=C_1f^{-m},\ \psi=\psi_1f^0. \tag{1}$$

Thus m and ψ are two empirical constants, characteristic of the polarization. Assuming that the exponent, m, is invariant with respect to the frequency, Fricke[1] has developed the relation

$$\psi=\pi m/2, \tag{2}$$

which is in good agreement with the available data. This makes it possible to describe the variation of the polarization with frequency in terms of a single parameter, m. The values of m found experimentally are in general equal to or less than 0.5.

The polarization impedance may be interpreted in terms of a variety of electrical networks. Of these the simplest are (1) a capacity C_s, in series with a resistance, R_s, and (2) a capacity, C_m, in parallel with a resistance, R_m. The values of the polarization capacity and resistance are not the same in the two cases but are connected by the relations

$$C_m=C_s\cos^2\psi,\ R_s=R_m\sin^2\psi, \tag{3}$$

in which $\psi=\tan^{-1}(2\pi fC_sR_s)=\cot^{-1}(2\pi fC_mR_m)$. A notation due to Wien which has been much used defines a polarization capacity $C_w=C_s\cos\psi=1/2\pi fz$ in which z represents the numerical value of the polarization impedance. If Eqs. (1) are valid when C represents any one of the quantities C_s, C_m or C_w, they are valid when it represents either of the other two. Another form[2] of the empirical law of Eqs. (1) is

$$z=(r^2+x^2)^{\frac{1}{2}}=(r_1^2+x_1^2)^{\frac{1}{2}}f^{-\alpha}=z_1f^{-\alpha}, \tag{4}$$

in which $r=R_s$ is the polarization resistance; $x=1/2\pi fC_s$, the polarization reactance; $\alpha=1-m$; and r_1, x_1 and z_1 are the values of r, x, and z, respectively, at unit frequency.

Wolff[3,4] has investigated the polarization of Pt-H_2SO_4-Pt cells through the wide range from $2\cdot10^2$ to $2\cdot10^5$ cycles per sec. For the higher values of electrolytic concentration, he finds that m increases with the frequency probably approaching the value, 0.5, found by Jolliffe[5] in the range from 10^5 to $2\cdot10^6$ cycles per sec. When the concentration is 0.2 N or less, Wolff finds no systematic variation of m with frequency. The purpose of this investigation was to extend the study of the polarization to very low

[1] H. Fricke, Phil. Mag. **14**, 310 (1932).

[2] Cf. K. S. Cole, Science **79**, 164 (1934).
[3] Irving Wolff, Phys. Rev. **27**, 755 (1926).
[4] Irving Wolff, article in this issue.
[5] C. B. Jolliffe, Phys. Rev. **22**, 293 (1923).

frequencies and to compare the results with those obtained by direct-current methods.

It is desirable to experiment with one cell through the whole range of frequencies. However, in order to obtain the desired sensitivity at low frequencies, one needs a cell with larger electrodes than those used by Jolliffe and Wolff. With the cell used in this investigation it was impractical to extend the measurements to frequencies above 3500 cycles per second. The electrodes were rectangular pieces of rolled platinum foil, having dimensions 1 cm by 0.75 cm, mounted in a parallel position with a separation of 0.54 cm. The electrolyte was a 0.25 N solution of sulphuric acid. All measurements were made at a temperature of 0°C after the cell had been conditioned so as to have its characteristic minimum polarization capacity. Only when a cell has been properly conditioned can measurements be duplicated with a sufficient degree of accuracy. The conditioning has usually been accomplished by allowing the cell to stand short-circuited for a long time. The procedure followed in these experiments was one previously used by Zimmerman.[6] The method consists in heating the cell from 0°C to 95°C, cooling it again to 0°C and then repeating the procedure as many times as necessary in order that the capacity shall come to the same value at 0°C after each heating. Two or three heatings are usually sufficient. The method is effective and avoids the long delay incident to the usual conditioning process. After the cell had been conditioned it was maintained at a temperature of zero degrees and the electrodes were kept shorted except while measurements were being made.

The measurements at frequencies ranging from 60 to 3500 cycles per second were made by means of an audiofrequency impedance bridge. Excepting the measurement at 60 cycles per second, the apparatus and procedure were the same as in work previously described by one of the authors.[6] In the measurement at 60 cycles per second, a vibration galvanometer replaced the ear phones as a detector.

The measurements of polarization capacity at low frequencies were made with an Einthoven string galvanometer connected in series with the cell, an adjustable resistance and a source of sinusoidal electromotive force. The current through the galvanometer was recorded as a function of time on a moving photographic plate. The shadow of a fine pointer operated electromagnetically by a half seconds pendulum fell on one edge of the plate and gave a time record. A similar pointer placed so that its shadow fell upon the other edge of the plate was actuated whenever the electromotive force attained its maximum positive value. It was thus possible from the photographic record to determine the frequency and amplitude of the alternating current and the phase difference between it and the impressed electromotive force.

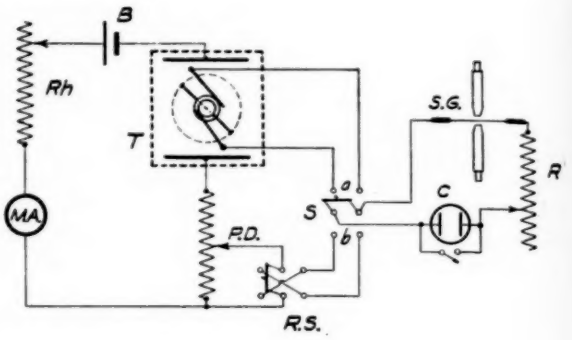

FIG. 1. Diagram of connections.

A schematic diagram of the electrical connections is shown in Fig. 1. A lead storage cell, B, was in series with an adjustable rheostat, Rh, a potential divider, $P.D.$, a milliammeter and a Cu-$CuSO_4$-Cu cell. The electrodes of this cell were heavy copper plates about one foot apart and designed to produce a current of uniform density in the solution. A shallow tray, T, served as the container for the electrolyte. Over the center of the tray a vertical shaft was mounted so that it could be rotated through gears and a variable ratio friction drive by an electric motor. At its lower end, the shaft carried a horizontal wooden bar, 18 cm in length, underneath and at the ends of which two thin copper strips were fastened. These dipped into the solution and described a circular path therein as the vertical shaft was rotated. Leads connected the strips to slip rings from which connection was made through brushes to fixed terminals. By means of this apparatus an alter-

[6] E. E. Zimmerman, Phys. Rev. **35**, 543 (1930).

nating potential of the desired amplitude was available. If the circuit to which the rotating electrodes were connected was of sufficiently high impedance so that the current drawn in the circuit did not effectively alter the lines of flow in the solution, the potential difference between the moving electrodes was sinusoidal. The rotating member also carried an arm which made an electrical contact once a revolution. A circular scale enabled one to adjust this contact so that it occurred at any desired epoch of the revolution. In these experiments the adjustment was such that the contact occurred at the instant of maximum electromotive force and actuated the pointer to which reference is made above. The switch, *S*, made it possible to connect the circuit consisting of the string galvanometer, *S.G.*, the resistance, *R*, and the electrolytic cell, *C*, either (a) to the source of alternating potential or (b) to the terminals of the potential divider.

In exposing a plate, a record was first made of the alternating current with the switch *S* in position (a). When several complete oscillations had been recorded on the moving plate, the switch *S* was thrown to position (b) and the reversing switch, *R.S.*, was thrown back and forth several times. The record thus produced served as the galvanometer calibration. This apparatus was used for the frequency range from 0.05 to 1.1 cycles per second. The amplitude of the alternating potential could be varied by adjusting the rheostat and was never greater than 0.05 volt. It has been shown by several investigators that below this value the capacity is independent of the value of the polarization electromotive force.

For any one given frequency at which data were taken, three or four plates were exposed. One plate of each set was made with a relatively small resistance in series with the cell; another with the cell short-circuited and a resistance of such value as to give a current of about the same amplitude as on the first plate. The other plates of the set were exposed with the cell in series with larger values of the resistance. It was the original intention to expose one plate of each set with the value of the resistance, *R*, zero. This was found impracticable as the circuit then had characteristics approximating those of an impulsive network.[7] Small fluctuations in the value of the alternating potential, which were probably caused by imperfections in the driving geers, produced large erratic variations in the current. The smallest value of *R* actually used was such as to so reduce these fluctuations as to make them negligible.

The alternating current records were in general sinusoidal within the accuracy of measurement. The occasional distortions were all associated with a failure of the rotating mechanism to maintain uniform motion. The sinusoidal curves obtained when the cell was replaced by a resistance are evidence that the electromotive force was sinusoidal. Those obtained with the electrolytic cell in place show that the cell produced no distortion of wave form.

Since the potential divider and the source of alternating potential were both actuated by the same direct current, it was not necessary to measure this current accurately but only to keep it constant. The value of the amplitude of the alternating potential could be computed in terms of the potential divider readings either from any plate exposed when the cell was short-circuited or from any two plates exposed with the cell in the circuit provided the frequency was the same. The results by the two methods were in good agreement.

Excepting the value of the series resistance, and the setting of the potential divider, all the data needed were recorded on the moving plate. From the maxima and minima of the sinusoidal record and the calibration record, the amplitude of the alternating current was computed. The times of maximum current were computed by the method of middle elongation and these, together with the times of maximum electromotive force, made possible the computation of the frequency of the alternating current and its lead angle. These data together with the value of the amplitude of the impressed potential completely determined the resistance and the reactance of the circuit. The reactance, thus determined, is the polarization reactance, x, since the reactance of the circuit exclusive of the cell is negligible. The polarization resistance, r, is obtained by subtracting from the circuit

[7] V. Bush, *Operational Circuit Analysis* (John Wiley and Sons, New York).

resistance the ohmic resistances in the circuit including the resistance of the electrolyte.

The results of the alternating current measurements are shown in Fig. 2 where the polarization reactance, x, and the polarization resistance, r, are plotted against frequency using logarithmic scales. The circles indicate mean values and are used when all the data at a given frequency are in substantial agreement. The crosses indicate individual measurements at frequencies at which the data are scattered. If the empirical law expressed by Eq. (4) is valid, the data for x and r should lie on two parallel straight lines of slope, $-\alpha$, and the ordinates of the lines should differ by $-\log \tan \psi$. If Fricke's relation is valid, ψ and therefore this difference in ordinate is determined by α. The reactance data in Fig. 2 are satisfactorily represented by the upper straight line. The slope gives $\alpha = 0.89$, $m = 0.11$ and by Eq. (2) $\psi = 10°$. The dash line is drawn parallel to the upper line with a difference in ordinates of $-\log \tan 10°$ in accordance with the Fricke relation and seems to represent the polarization resistance as well as possible for data subject to so much uncertainty.

The measurements of the polarization resistance in the low frequency range have large fractional errors because they are obtained by the subtraction of two larger quantities. In the audiofrequency range the polarization resistance is of the same order of magnitude as the resistance of the electrolyte and the effective value of this is not easily determined in a cell of the type used. The current density and consequently the polarization varies from point to point over the surface of the electrode and as a result the surface of the electrolyte adjacent to the electrode is not equipotential. This distorts the current stream lines in the electrolyte so as to increase the effective resistance. In Fig. 2 double pointed arrows are used to plot r in the audiofrequency region. The upper points indicate the value of r computed using 4.4 ohms as the resistance of the electrolyte. This is the resistance of the cell as measured by using platinized electrodes to eliminate the effects of polarization. These points are then upper limits to the value of the polarization resistance. In order to show the influence of the effective electrolytic resistance on the results at various frequencies the arrows are drawn so that their lower points indicate the result obtained when the cell resistance is taken as 8.0 ohms. The choice of this value is quite arbitrary, it being a crude estimate of an extreme value of the effective resistance of the electrolyte.

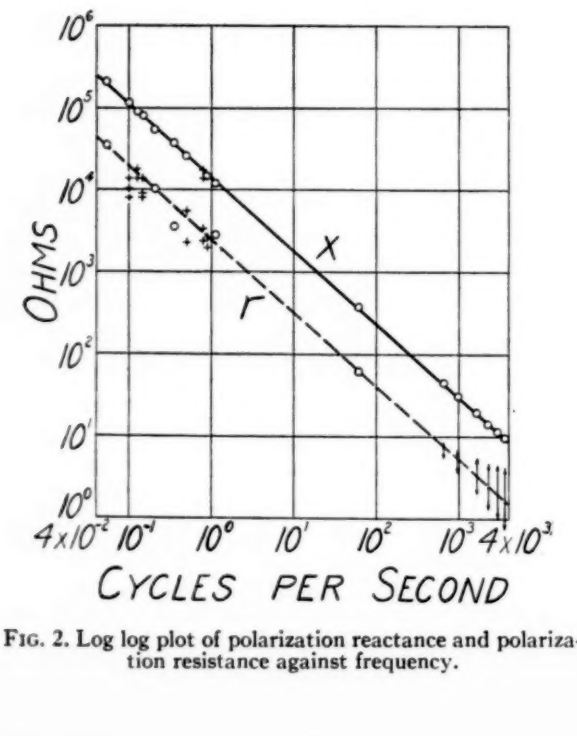

FIG. 2. Log log plot of polarization reactance and polarization resistance against frequency.

The uncertainty of the measurements at high and low frequencies makes it difficult to draw definite conclusions regarding the polarization resistance. However, the one point not seriously influenced by either type of error, *viz.* that at 60 cycles per second, lies very close to the line and the deviation of the points at either end are of the type to be expected in view of the nature of the errors involved. With a cell whose electrolyte had a concentration of 0.2 N, Wolff[3] found ψ and m constant in the range 650 to 3500 cycles per second and the design of his cell was such that the electrolytic resistance error was not effective at this frequency. From the data as shown in Fig. 2 we may conclude that m and ψ are independent of the frequency from audiofrequencies down to 0.05 cycle per second and that in this range they satisfy the Fricke relation. A more critical test of the constancy of m is shown in Fig. 3 in which C_w per square centimeter of each electrode is plotted against frequency using logarithmic scales. The values

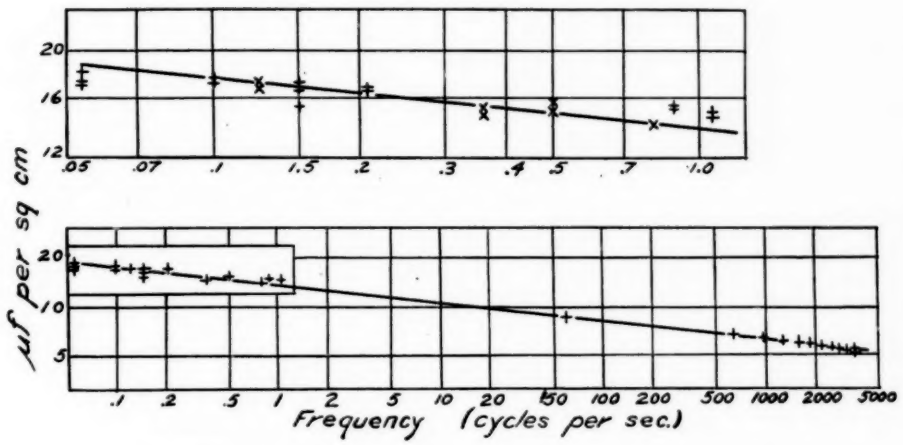

FIG. 3. Log log plot of polarization capacity, C_w, against frequency.

of C_w plotted in the upper bracket were each computed from a single photographic plate using the values of x and r as measured on that plate. They are therefore subject to the accidental errors of the measurement of r in that region.

If Eqs. (1) hold accurately for all frequencies, the polarization capacity is infinite at zero frequency. Direct-current methods of measuring polarization capacity have frequently been used and give finite results. One might expect the value of the polarization capacity obtained by a direct current method to depend upon the time constant of the circuit in a way similar to that in which the value as obtained by alternating current methods depends upon the period of the current. This question has been investigated by Pierce[8] who found no change in the polarization capacity of a Pt-H_2SO_4-Pt cell when the time constant of the circuit varied through the range 1 to 2.4 seconds.

The apparatus shown in Fig. 1 served very conveniently for making direct-current measurements by the method that Pierce used. With the switch, S, in position (b), the reversing switch was thrown while the photographic plate was moving across the field of the galvanometer. After the throw, the current as recorded on the plate suddenly increased and then slowly decreased tracing a curve which closely approximates an exponential decay curve asymptotic to a line parallel to the time axis.

The record on the plate may be interpreted by considering that the electrolytic cell is equivalent to a capacity, C_m, and a resistance, R_m, connected in multiple. The result with this network would be an exponential transient current of time constant, τ, superimposed upon a constant current, I_r, in accordance with the equations,[9]

$$I_r = E/R_m(1+\rho) \text{ and } \tau = RC_m/(1+\rho), \quad (5)$$

in which E is the impressed electromotive force, R is the ohmic resistance of the circuit and $\rho = R/R_m$. The effective values of I_r and τ were determined from the record on the plate. An approximate value of I_r was assigned by inspection and log $(I-I_r)$ was plotted as a function of time. In general, this line had a slight curvature. Different values of I_r were then tried until a straight line was obtained. The slope of this line gave the value of τ. All the quantities entering into Eqs. (5) were now known except C_m and R_m which were thus determined.

The values obtained for R_m by this method have low accuracy because of the large fractional error in the measurement of the very small residual current. They are not independent of R. The ratio $\rho = R/R_m$ has values 0.025, 0.042, and 0.055 for $R = 10{,}000$, 42,000, and 82,000 ohms, respectively. The crosses in Fig. 4 show the values of the time constant, τ, plotted against $R/(1+\rho)$. If C_m is independent of the time constant, the points should be upon a straight line through the origin. They do in fact lie close to

[8] W. M. Pierce, Phys. Rev. **31**, 470 (1928).

[9] C. C. Murdock, Phys. Rev. **17**, 633 (1921).

such a line whose slope would correspond to the result, $C_m = 13.6$ microfarads.

In analyzing the direct-current data we have regarded the current as the sum of a steady state current, I_r, and a transient current from the decay of which we determined C_m. An alternating electromotive force similarly produces a current which is the sum of a steady state alternating current and a transient current. The points indicated by the small circles in Fig. 4 show the results of a study of alternating current transients. The procedure was the same as in the alternating current measurements previously described except that switch S was opened after about two cycles of the steady state current had been recorded and again closed at about the time of the next electromotive force maximum. The resulting transient current is of measurable magnitude immediately after the closing of the switch, but becomes negligible before the end of the record. One plate of this sort was made in each of several of the sets. Particular care was taken in determining the parameters of the steady state alternating current from the records at the extremities of these plates. The values of the steady state current were computed for the region of the transient and subtracted from the observed values of the current to give the transient current. The time constant was then determined by the same method as in the direct-current measurements.

Although the data of Fig. 4 lie close to a straight line, there is evident a systematic deviation as indicated by the dash line. Since the value of C_m for any point is, by Eq. (5), the slope of the straight line from the origin to that point, Fig. 4 indicates that the values of C_m as measured increase with R, that is, with the time constant of the circuit. The variation is so slight that it is not surprising that Pierce did not observe it within the range of time constant which he used.

In the experiment involving the analysis of the alternating current transients we have in a sense simultaneously made two measurements of the polarization capacity, one at a definite frequency and the other with an aperiodic current. The fact that in Fig. 4 the points representing data obtained from the alternating-current transients fall so closely in line with those from the aperiodic current measurements, indicates that the measurement of the polarization capacity by an aperiodic current is not influenced by the simultaneous transmission by the cell of a periodic current. Wolff[10] has found experimentally that the value of the polarization capacity measured at one frequency is not affected by the presence of an alternating current of another frequency. Our results justify the extension of this superposition principle to include aperiodic currents.

The alternating-current experiments have verified the law of frequency variation of polarization impedance down to frequencies so low that the period of alternation is of the same order of magnitude as the time constant of the circuit with which the aperiodic current experiments were performed. This makes it possible to predict the aperiodic current as a function of time in terms of the alternating-current results by the use of Fourier series and to compare the aperiodic current results with those obtained with the same cell by alternating currents. The development throws some light upon the interpretation of data taken by aperiodic methods.

Let us consider, first, the case in which the current is observed while the reversing switch is thrown periodically with a constant period of

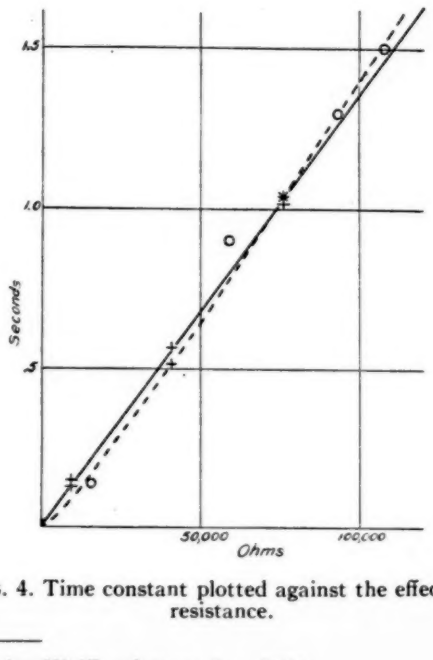

FIG. 4. Time constant plotted against the effective resistance.

[10] Irving Wolff, reference 3, p. 760.

$2\pi/p$. The impressed electromotive force is alternately E and $-E$. A periodic electromotive force of this type may be represented by the Fourier series

$$e=\sum_n\{[4E/(n\pi)]\sin(npt)\},\quad n=1,3,5\cdots. \tag{6}$$

Each term of this series is a sinusoidal electromotive force and from the results of the alternating-current experiments the values of the polarization resistance and reactance corresponding to the frequency of each term are known. If the ohmic resistance of the circuit, R, is also known the sinusoidal current which each term of the series would by itself produce is determined. By the principle of superposition, the sum of these is the resultant current,

$$i=\sum_n\{[4E/(n\pi((R+r)^2+x^2)^{\frac{1}{2}})]\sin(npt+\phi)\},\quad n=1,3,5,\cdots,$$

in which $\phi=\tan^{-1}[x/(R+r)]=\cot^{-1}[(R/x)+\tan\psi]$. If now we express r and x in terms of the empirical constants by Eqs. (3) and (4), we obtain

$$i=\sum_n\{[4E\cos\phi(1-\tan\psi\tan\phi)/(n\pi R)]\times\sin(npt+\phi)\},\quad n=1,3,5\cdots, \tag{7}$$

and
$$\phi=\cot^{-1}[(2\pi)^m C_{1s}R(np)^\alpha+\tan\psi], \tag{8}$$

in which $np=2\pi f$, the angular frequency of the nth harmonic of the series. The polarization electromotive force, ϵ, is equal to $e-Ri$ by Kirchhoff's law and by Eqs. (6) and (7) we obtain

$$\begin{aligned}\epsilon&=\sum_n\{[4E/(n\pi)][\sin(npt)-(\cos\phi-\tan\psi\sin\phi)]\sin(npt+\phi)\}\\&=-\sum_n\{[4E\sin\phi\sec\psi/(n\pi)]\times\cos(npt+\phi+\psi)\},\quad n=1,3,\cdots.\end{aligned} \tag{9}$$

The functions e and i have finite discontinuities when t is an integral multiple of π/p and the two series in Eqs. (6) and (7) do not represent the functions at these values of t. However the polarization electromotive force, ϵ, is essentially continuous and Eq. (9) holds at all values of t. The value of the polarization, ϵ, at time $t=0$ is therefore

$$\epsilon]_{t=0}=-\sum_n[4E\sin\phi(\cos\phi-\tan\psi\tan\phi)/(n\pi)]. \tag{10}$$

We have here discussed the case of the alternating current produced by an electromotive force of constant value but alternating as to sign. Considering only a single half period, we may describe this case as that of a decay current produced by a constant electromotive force when the initial polarization of the cell is given by Eq. (10). Consider now the more general case in which the electromotive force, E, is impressed upon the cell when the polarization of the cell has some given value, ϵ_0, such that if we substitute ϵ_0 for ϵ in Eq. (9) we find that equation satisfied if t has some value, t_0, which lies in the range, $0\leqq t_0\leqq\pi/p$. Since within this range the current, i, is a single valued function of E, ϵ, and R, the subsequent decay of the current will be the same as if the process had started at time $t=0$ when the polarization was that given by Eq. (10). Therefore if we substitute (t_0+t') for t in Eq. (7) it will give the value of the decay current in the time range, $0\leqq t'\leqq(n/p)-t_0$ for the case in which an electromotive force, E, is impressed at a time, $t'=0$, when the polarization electromotive force is ϵ_0, the value of t_0 being found by solving Eq. (9) for t after the substitution of ϵ_0 for ϵ.

We have developed an expression, in terms of the parameters determined by the alternating-current measurements, for the current which results when a constant electromotive force is impressed upon an electrolytic cell. Experimentally it is found that the value of this current may be represented within the accuracy of measurement as the sum of a constant residual current and an exponential decay current such as would occur in a circuit in which the resistance, R, is in series with the multiple connection of a resistance, R_m, and a capacity, C_m. The problem of the behavior of such a circuit under the action of an impressed electromotive force, E, may also be solved in terms of Fourier series by an argument analogous to that given above. The results are

$$j=\sum_n\{[4EnpC_m\sec^2\xi\sin\theta/(n\pi)]\times\sin(npt+\theta)\},\quad n=1,3,\cdots, \tag{11}$$

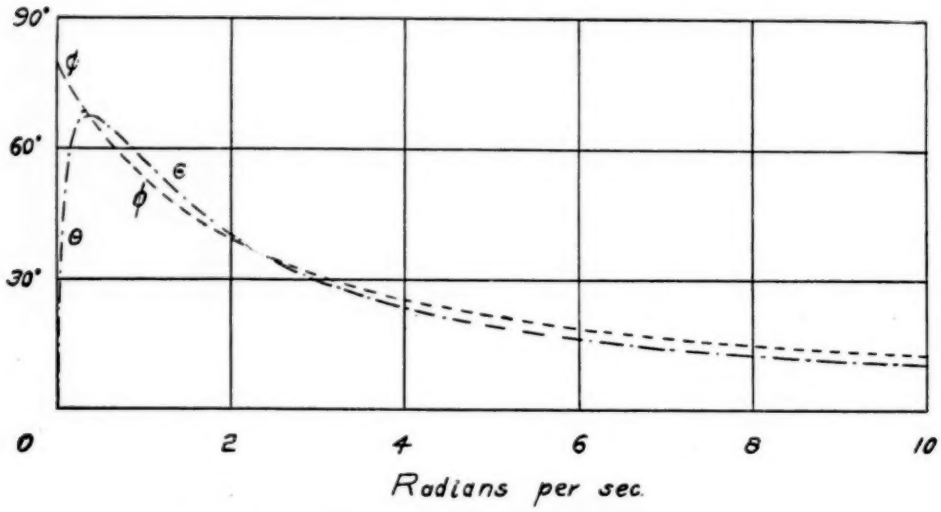

FIG. 5. Phase angles θ and ϕ plotted against angular frequency.

$$v_0 = -\sum_n \{[4E \sec \xi \sin \theta/(n\pi)] \times \cos (npt_0 + \theta + \xi)\}, \quad n = 1, 3, \cdots, \quad (12)$$

in which v_0 is the potential difference of the condenser at time $t' = 0$, j is the current at time t', $t = t_0 + t'$, t_0 being determined by Eq. (12), $\xi = \tan^{-1} [\rho/(npRC_m)]$, and

$$\theta = \cot^{-1} [npRC_m + (1+\rho) \tan \xi]. \quad (13)$$

The expression for i becomes identical with that for j if m is zero, $(\alpha = 1)$, but when m is finite, no values of C_m and ρ can be found which substituted in Eq. (11) will make the Fourier series for j and i identical term by term. It follows that if Eqs. (1) and (2) are correct, our interpretation of the experimental results in terms of definite values of C_m and ρ is based upon an approximation.

A comparison of Eqs. (7) and (11) shows that if j is to approximate i, θ must be nearly equal to ϕ over a wide frequency range. That this is the case when $R = 42{,}000$ ohms $(\rho = 0.042)$ is shown by Fig. 5 in which ϕ and θ are plotted as functions of the angular frequency, np, using the experimentally determined values of m, α, C_{1s}, ψ and C_m. These curves are typical of those obtained using other values of R. Both ϕ and θ approach the frequency axis asymptotically but while ϕ decreases with increasing frequency from a value $\pi/2 - \psi$, θ increases from zero to a maximum at $np = (\rho(1+\rho))^{\frac{1}{2}}/RC_m$ and then decreases through a point of inflection at $np = (\rho(1+\rho))^{\frac{1}{2}}/RC_m$. Values of C_m and ρ may be found which will approximately superimpose the two curves in the neighborhood of the inflection point and for all larger values of the angular frequency but the two curves will differ widely for values of np less than that of the maximum. A necessary condition for an approximate interpretation in terms of C_m and ρ is therefore $np > (\rho(1+\rho))^{\frac{1}{2}}/RC_m$ or since ρ is small and n is any odd integer, $p > \rho^{\frac{1}{2}}/RC_m$. By assuming this condition, the amplitude of the nth harmonic of the Fourier series of Eq. (11) may be developed in terms of powers of ρ giving

$$j = \sum_n \{[4E \cos \theta (1 - \rho \tan^2 \theta - \cdots)/(n\pi R)] \times \sin (npt + \theta)\}, \quad n = 1, 3, \cdots. \quad (14)$$

A comparison of this expression with Eq. (7) shows reason to expect the approximate equality of i and j which has been found experimentally. In both series the amplitudes approach the value $4E/(n\pi R)$ as the frequency increases. Throughout the frequency range in which θ is approximately equal to ϕ, $\cos \theta$ is nearly equal to $\cos \phi$, since the angles are in general less than 60°. The terms $\tan \psi \tan \phi$ and $\rho \tan^2 \theta$ are small compared with one and are important only at small values of n at which the requirement is that $\rho \tan \theta$ shall be of the same order of magnitude as

$\tan \psi$. These conditions have been checked using the experimental data corresponding to three points of Fig. 4 and have been found to hold.

The value of the current, i, at time, t', as expressed by Eq. (7) for the time interval $0 \leqq t' \leqq (\pi/p) - t_0$ is independent of the value of p. The same is true of j similarly expressed by Eq. (14). However, j approximates i only if p is greater than $\rho^{\frac{1}{2}}/(RC_m)$ or since RC_m is nearly equal to the time constant, τ, $p > \rho^{\frac{1}{2}}/\tau$. Thus the region in which the approximation is good is $0 \leqq t' \leqq (\pi\tau/\sqrt{\rho}) - t_0$. This does not interfere with the experimental determination of C_m because before the time limit is exceeded the current becomes too small for accurate measurements. It does, however, indicate that at values of t' greater than $(\pi\tau/\sqrt{\rho}) - t_0$ the current will not approach the value I_r, and we have frequently observed that the current ultimately decays to values less than those obtained for I_r.

Eqs. (7), (8), and (9) determine the current decay law and we may from them deduce the nature of the variation of τ and C_m with respect to R. Multiply Eq. (7) through by R, giving a Fourier series expression for Ri, the potential difference across the resistance, R. Both this series and that of Eq. (9) are independent of R except as they depend upon ϕ. The sums of these series are also independent of the fundamental angular frequency, p. Suppose that the value of R is now changed by an arbitrary factor, s^α, and that we simultaneously change p by the factor, s^{-1}. The product Rp^α which occurs in Eq. (8) is unchanged and the phase angle, ϕ, of each term of the two series is the same as before. Now Ri and e are single valued varying functions of time and their values have not been affected by the changes in R and p. It follows that the angle (npt) of each term of the two series must also be unchanged. Since p has been multiplied by s^{-1} this requires that t be multiplied by s. Thus in changing the resistance, R, by a factor, s^α, we have changed the functions (Ri) and ϵ only by changing the time scale by the factor s. The time interval, t', which must elapse after the time t_0 at which $\epsilon = \epsilon_0$ and $Ri = Ri_0$ before Ri becomes equal to any specified value is changed by the factor s. If this specified value of Ri is $Ri_0/2.72$, t' is by definition the time constant, τ. Thus the time constant as measured is proportional to $R^{1/\alpha}$. The dash line in Fig. 4 is drawn in accordance with this condition and satisfactorily represents the data.

Since $1+\rho$ varies only slightly with R we obtain from Eq. (5) the approximate relation, $C_m \propto \tau/R \propto \tau/\tau^\alpha = \tau^{1-\alpha} = \tau^m$. This result is analogous to the empirical law of Eq. (1) which may be written $C \propto T^m$ in which T is the period of the alternating current. We have arrived at this result by the consideration of the form of the decay current curve. If C_m is measured by the more usual method of the ballistic galvanometer, the result is the same. Here C_m is approximately proportional to the area of the current decay curve. The ordinates of this curve are proportional to R^{-1}, the abscissa $R^{1/\alpha}$, and the area to $R^{m/\alpha}$, that is to τ^m.

The alternating-current method of investigating electrolytic polarization is unquestionably more accurate than the direct-current method. It appears that the values of polarization capacity obtained by the latter method are not limits approached as the frequency approaches zero, but depend upon the time constant of the circuit by a relation analogous to the empirical law which holds for alternating-current measurements.

Radiation from an Antenna Over a Plane Earth of Arbitrary Characteristics

W. W. HANSEN AND J. G. BECKERLEY, *Department of Physics, Stanford University*

(Received April 13, 1936)

A rigorous and easily computed formula for the total radiation from an arbitrary current distribution above a plane "earth" of arbitrary characteristics is developed. The fields may also be found, though they are not needed to compute the energy radiated. As a by-product, two new expansions in cylindrical coordinates of $\mathbf{i}(1)e^{ikr_{12}}/r_{12}$, where $\mathbf{i}(1)$ is a vector, are found.

THE principal result of the present paper may be expressed qualitatively as follows. A set of orthogonal vector functions is found such that if one expands any current distribution in a series of these functions the sum of the squares of the expansion coefficients is a measure of the energy radiated from the current distribution; and the same formulae apply if there is an "earth" of arbitrary characteristics below the distribution. Thus the present analysis solves the problem of computing the radiation from a radio antenna. In addition to finding the total radiation it is found possible to compute the fraction of the energy that is eventually absorbed in the medium. We also find as a special case a formula in cylindrical coordinates that enables one to compute the total radiation from an arbitrary current distribution in free space. Finally, we use the vector functions introduced for the solution of the radiation problem to make up two new vector expansions of $\mathbf{i}(1)e^{ikr_{12}}/r_{12}$.

To be more exact as to the problem, we divide space into two parts bounded by the plane $z=0$; for $z>0$ the quantities μ, ϵ, σ (permeability, dielectric constant, conductivity) have the values 1, 1, 0, respectively, which correspond to free space, and for $z<0$ the same quantities have arbitrary constant values. We assume the current to be confined to a finite region in $z>0$. Then we try to find fields which satisfy the correct wave equations above and below the ground, which do the proper things at infinity and which correspond to the given current distribution. Finally from these fields we want to find the total radiation. Of course the fundamental principles involved have been known since the time of Maxwell, so that the problem is the purely mathematical one of finding such fields and the radiated energy and doing it in such a way that the final results will be in a form simple enough to use. Thus if there is no ground one can at once write a formal answer to the problem involving an eightfold integral of current times $e^{ikr_{12}}/r_{12}$, etc., but this is hardly a practical solution. More or less obvious devices can be used to reduce the problem to one involving five integrations. Three of these arise in finding the fields by means of retarded integrals, the remaining two come from integrating the Poynting vector over all directions. In the present work the last two integrations are avoided. Instead one finds "oscillator strengths" by means of volume integrals and then sums (or integrates) squares of these.

To effect the solution of the problem proposed we combine two previously used methods[1, 2] as follows. The presence of the boundary at $z=0$ obviously requires either Cartesian or some form of cylindrical coordinates; we choose circular cylinders as being the most convenient, although either of the other separable cylindrical coordinates or Cartesian coordinates could be used. We now consider the vector potential due to that part of the current in a lamina of thickness Δz. To do this we further subdivide the current by expressing the current in the chosen lamina as a sum of a series of orthogonal vector functions. The vector potential associated with one term of the expansion is now easily found by the solution of a simple boundary value problem; the presence of the ground is simultaneously taken into account by the use of the same methods. We next find the complete vector potential by summing over the terms of the expansion in orthogonal functions and integrating over the various laminae. Because of the choice of functions it is found easy to compute the fields and it remains only to find the Poynting

[1] W. W. Hansen, Phys. Rev. **47**, 139 (1935).
[2] W. W. Hansen, Proc. Nat. Acad. Sci. **21**, 326 (1935).

vector and integrate it over a closed bounding surface. This process is easy because orthogonality relations eliminate cross product terms and make it possible to write the final results in simple form.

To carry through the above proposed process we will need various functions, which we now define. The three functions[3]

$$\mathbf{A}^+_{1,\,n}=\nabla\xi_n,$$
$$\mathbf{A}^+_{2,\,n}=\nabla\times\mathbf{k}_z\xi_n=(1/k)\nabla\times\mathbf{A}^+_{3,\,n}, \qquad (1)$$
$$\mathbf{A}^+_{3,\,n}=(1/k)\nabla\times\mathbf{A}^+_{2,\,n},$$

with

$$\xi_n=e^{i(mz+n\phi)}J_n(lr), \quad m=+(k^2-l^2)^{\frac{1}{2}} \qquad (1a)$$

are three solutions of the vector wave equation with the time factor removed.[4]

It is useful to consider these functions as consisting of two factors. Thus we let

$$\mathbf{A}^+_{1,\,n}(r,\phi,z:l)=e^{imz}\mathbf{a}^+_{1,\,n}(r,\phi:l), \quad \text{etc.} \qquad (2)$$

define vector functions $\mathbf{a}_1^+$, $\mathbf{a}_2^+$, $\mathbf{a}_3^+$.

We will also use functions defined in the same way but with the e^{imz} of ξ replaced by e^{-imz}; these we denote by $\mathbf{A}^-$ and $\mathbf{a}^-$. The important property of the functions $\mathbf{a}$ so defined is that they form a complete orthogonal set of vector functions. Thus we have for both the plus and minus sets of $\mathbf{a}$'s

$$\int_0^{2\pi}\int_0^{\infty}\int_0^{\infty}\mathbf{a}_{1,\,n}(r,\phi:l)\cdot\bar{\mathbf{a}}_{1,\,n}(r,\phi:l')l'dl'rdrd\phi=2\pi k^2,$$
$$\int_0^{2\pi}\int_0^{\infty}\int_0^{\infty}\mathbf{a}_{2,\,n}(r,\phi:l)\cdot\bar{\mathbf{a}}_{2,\,n}(r,\phi:l')l'dl'rdrd\phi=2\pi l^2, \qquad (3)$$
$$\int_0^{2\pi}\int_0^{\infty}\int_0^{\infty}\mathbf{a}_{3,\,n}(r,\phi:l)\cdot\bar{\mathbf{a}}_{3,\,n}(r,\phi:l')l'dl'rdrd\phi=2\pi l^2.$$

All other integrals of this type vanish. As is usual in Fourier integrals the relevant region of integration over l' is an infinitesimally narrow one centered on $l'=l$. Some of these integrals can be evaluated by using the explicit forms of the functions found by working (1) out in cylindrical coordinates. But in some of them, notably the one (which comes to zero) involving the product $\mathbf{a}_1\cdot\mathbf{a}_3$, the use of Cartesian components of the $\mathbf{A}$ is almost essential. These may be obtained by direct transformation of the polar components and skillful use of Bessel function recursion formulae, or, more elegantly, by representing ξ in Whittaker's form and noting that $\partial/\partial x$, $\partial/\partial y$, and $+\partial^2/k\partial x\partial z$ operating on ξ lead to the x components of $\mathbf{A}_1$, $\mathbf{A}_2$, and $\mathbf{A}_3$. These operators, and the similar ones giving other components, may be passed under the integral sign in Whittaker's formula, and the needed components are found at once.[5]

Of the many properties of the functions $\mathbf{A}$, etc., we may note the following. The curl of $\mathbf{A}_1$ is zero, while the divergences of $\mathbf{A}_2$ and $\mathbf{A}_3$ vanish. Thus any electric or magnetic field in free space is expressible in terms of $\mathbf{A}_2$ and $\mathbf{A}_3$ only. The vector potential may contain terms in $\mathbf{A}_1$, but in computing the electric field these will just cancel against terms from the scalar potential. We may also observe that, for $n\geq 1$, $\mathbf{A}_2$ and $\mathbf{A}_3$ are the cylindrical counterparts, respectively, of the ordinary magnetic and electric dipole, quadrupole, etc. The case $n=0$ has no parallel in spherical coordinates; it is possible to construct an axially symmetric solution of a vector wave equation but not a spherically symmetric one. We also note that with increasing n the various functions vanish like higher powers of r at the origin. It is for this reason that the series of oscillator strengths used later converges rapidly.

Finally we must consider how the various boundary conditions are to be met at $z=0$, i.e., at the ground. This we do by always using in connection with any given $\mathbf{A}^-$ a reflected wave made up of solutions $\mathbf{A}^+$ with proper coefficients. The coefficients are determined by requiring that proper boundary conditions be satisfied at the ground. On calculation, six of the nine possible coefficients are found to vanish and the

[3] This is not the only possible triad of functions that might be used. For example the three functions $k\mathbf{k}_z\xi$, $(l^2/k)\mathbf{A}_1-im\mathbf{A}_3$ and $\mathbf{A}_2$ will be found to be a fairly usable set.

[4] As to notation: r, ϕ, z are the standard cylindrical coordinates; vectors are in bold face; $\mathbf{k}_z$ is a unit vector in the z direction; and k is the "wave number" $2\pi\nu/c$. The time factor is taken to be $e^{-i\omega t}$ so that the above is a wave running in the positive z direction.

[5] The exact form for ξ is not given in Whittaker and Watson (*Modern Analysis*, fourth edition) but is easily found from the equations of (18.5).

proper wave for $z>0$ can be written in the form $\mathbf{A}_s^- + \alpha_s \mathbf{A}_s^+$.[6] The actual values of the "reflection coefficients" are

$$\alpha_1 = (m-m')/(m+m'),$$
$$\alpha_2 = (\mu m - m')/(\mu m + m'), \tag{4}$$
$$\alpha_3 = (\epsilon' m - m')/(\epsilon' m + m'),$$

with $\epsilon' = \epsilon + i\sigma/kc$ and $m'^2 = k^2\epsilon'\mu - l^2$. In the ground the wave function involves $e^{-im'z}$ and m' is usually complex with the result that the wave is exponentially damped. Though the function is easily found, it is not given as we never find use for it.

With the functions defined above we can proceed with the program outlined in the introduction. We consider for a moment only that part of the current lying between z' and $z'+dz'$ and this we expand in a series of the vector functions $\mathbf{a}^-$. The expansion coefficients will of course depend on z'. Thus we write

$$\mathbf{i}(r', \phi', z') = \sum_s \sum_n \int_0^\infty b^-_{s,n}(z' : l)\mathbf{a}^-_{s,n}(r', \phi' : l)\,l\,dl \tag{5}$$

where the summation over n is from minus infinity to plus infinity. We have used primed coordinates for the location of the current; the unprimed coordinates will be used presently for the point at which the fields are desired. Multiplying this equation by $\bar{\mathbf{a}}^-_{s,n}$ and integrating over r' and ϕ', one finds on using (3)

$$b_{1,n}(z' : l) = (1/2\pi k^2)\int\int \mathbf{i}(r', \phi', z')\cdot\bar{\mathbf{a}}^-_{1,n}(r', \phi' : l)\,r'\,dr'\,d\phi',$$
$$b_{2,n}(z' : l) = (1/2\pi l^2)\int\int \mathbf{i}(r', \phi', z')\cdot\bar{\mathbf{a}}^-_{2,n}(r', \phi' : l)\,r'\,dr'\,d\phi', \tag{6}$$
$$b_{3,n}(z' : l) = (1/2\pi l^2)\int\int \mathbf{i}(r', \phi', z')\cdot\bar{\mathbf{a}}^-_{3,n}(r', \phi' : l)\,r'\,dr'\,d\phi'.$$

We now find the vector potential associated with a single term of the expansion of that part of the current lying in a lamina $\Delta z'$. This partial vector potential which we will call ΔA is uniquely determined by requiring that it shall (a) satisfy the homogeneous wave equation except in $\Delta z'$, (b) represent, at large distances, waves traveling toward infinity, and (c) be continuous at the current lamina but with a discontinuity in derivative of the proper magnitude.[7] The requirements force us to take

$$\Delta A = \frac{1}{2imc} b_{s,n}(z' : l)[e^{imz}\mathbf{a}^-_{s,n}(r, \phi : l) + \alpha_s(l)\mathbf{A}^+_{s,n}(r, \phi, z : l)]\,l\,dl\,\Delta z', \quad z' < z,$$
$$\Delta A = \frac{1}{2imc} b_{s,n}(z' : l)[\mathbf{A}^-_{s,n}(r, \phi, z : l) + \alpha_s(l)\mathbf{A}^+_{s,n}(r, \phi, z : l)]\,l\,dl\,\Delta z', \quad z' > z > 0. \tag{7}$$

We can now, by summation over s, n, and integration over l, find the vector potential due to the lamina; the complete vector potential is found by a further integration over z', which adds the effects of the laminae. So we find

$$A(r, \phi, z) = \frac{1}{2ic}\sum_s\sum_n\int_0^\infty [f^-_{s,n}(l)\mathbf{A}^-_{s,n}(r, \phi, z : l) + \alpha_s(l) f^-_{s,n}(l)\mathbf{A}^+_{s,n}(r, \phi, z : l)]\frac{l}{m}dl, \tag{8a}$$

which is valid between the lowest current element and $z=0$. To write A in this form we have introduced the "oscillator strengths" $f^-_{s,n}$. These and the $f^+_{s,n}$ to be used in a moment are defined as follows:

[6] For the index running from 1 to 3, which distinguishes the different types of $\mathbf{A}$'s we will use s. The index n is here suppressed as the α do not depend on n.

[7] We use Heaviside-Lorentz units.

$$f^{+}{}_{1,\,n}(l)=\frac{1}{2\pi k^2}\int\int\int \mathbf{i}\cdot\bar{\mathbf{A}}^{+}{}_{1,\,-n}(r',\,\phi',\,z'\,:\,l)r'dr'd\phi'dz',$$

$$f^{+}{}_{2,\,n}(l)=\frac{1}{2\pi l^2}\int\int\int \mathbf{i}\cdot\bar{\mathbf{A}}^{+}{}_{2,\,-n}(r',\,\phi',\,z'\,:\,l)r'dr'd\phi'dz', \tag{9}$$

$$f^{+}{}_{3,\,n}(l)=\frac{1}{2\pi l^2}\int\int\int \mathbf{i}\cdot\bar{\mathbf{A}}^{+}{}_{3,\,-n}(r',\,\phi',\,z'\,:\,l)r'dr'd\phi'dz'.$$

The expressions for $f^{-}{}_{s,\,n}$ are similar[8] except that $\bar{\mathbf{A}}_{-n}{}^{+}$ is replaced by $\bar{\mathbf{A}}_{-n}{}^{-}$. For the field above the uppermost current we might use an expression derived from the part of (7) suitable for $z>z'$. It is neater, however, to start anew and expand $\mathbf{i}$ in terms of the functions $\mathbf{a}^{+}$. This leads to

$$A=\frac{1}{2ic}\sum_{s}\sum_{n}\int_{0}^{\infty}(f^{+}{}_{s,\,n}+\alpha_s f^{-}{}_{s,\,n})\mathbf{A}^{+}{}_{s,\,n}\frac{l}{m}dl, \quad z>z'. \tag{8b}$$

Because of the definition of the $\mathbf{A}$'s the computation of fields is very simple. Thus if we curl (8) to find $\mathbf{B}$, the terms in $\mathbf{A}_1$ drop out and there is an interchange of indices 2 and 3. The electric field is found with equal ease. For example for z above all currents

$$\begin{aligned}\mathbf{B}&=\frac{k}{2ic}\sum_{n}\int_{0}^{\infty}[(f^{+}{}_{3,\,n}+\alpha_3 f^{-}{}_{3,\,n})\mathbf{A}^{+}{}_{2,\,n}+(f^{+}{}_{2,\,n}+\alpha_2 f^{-}{}_{2,\,n})\mathbf{A}^{+}{}_{3,\,n}]\frac{l}{m}dl,\\ \mathbf{E}&=\frac{k}{2c}\sum_{n}\int_{0}^{\infty}[(f^{+}{}_{2,\,n}+\alpha_2 f^{-}{}_{2,\,n})\mathbf{A}^{+}{}_{2,\,n}+(f^{+}{}_{3,\,n}+\alpha_3 f^{-}{}_{3,\,n})\mathbf{A}^{+}{}_{3,\,n}]\frac{l}{m}dl.\end{aligned} \tag{10}$$

We can now compute the Poynting vector and integrate this over a closed surface to find the power radiated. This surface we may conveniently take to be a right cylinder of large diameter with base just above the ground and top anywhere above the current distribution. We then need the z component of the Poynting vector over the two large disks and the r component over a cylinder of large radius. Because the functions used give waves that run only in the z direction, the r component oscillates and its average is zero. Because of the orthogonality of the $\mathbf{a}$'s it is found that on integrating the Poynting vector over the large disks all cross product terms disappear and the answer is essentially an integral over l of the squares of oscillator strengths. Moreover the term in $|\alpha_s f_s^{-}|^2$ cancels because it represents the same amount of energy entering the bottom and leaving the top of the cylinders. On the other hand, the cross product term, which corresponds to interference between direct and reflected up-going waves, survives. The result is

$$\begin{aligned}\int\mathbf{S}\cdot d\sigma=\frac{\pi k}{4c}\sum_{n}\int_{0}^{k}[&|f^{+}{}_{2,\,n}|^2\\ &+2R(\bar{f}^{+}{}_{2,\,n}\alpha_2 f^{-}{}_{2,\,n})+|f^{-}{}_{2,\,n}|^2+|f^{+}{}_{3,\,n}|^2\\ &+2R(\bar{f}^{+}{}_{3,\,n}\alpha_3 f^{-}{}_{3,\,n})+|f^{-}{}_{3,\,n}|^2]\frac{l^3}{m}dl.\end{aligned} \tag{11}$$

Here $\mathbf{S}$ is the time average of the Poynting vector and R means "the real part of."

It is to be noted that the upper limit here is not infinity, but k. This is so because when $l>k$ the wave number in the z direction is imaginary so that there are no longer waves running in the z direction, and the time average of this component of the Poynting vector vanishes. Such waves with an excessive wave number in one direction and exponential damping in another are exactly like the waves in the less dense medium under conditions of total internal reflection. We recall that in this case no energy is carried into the less dense medium.

[8] Because of the relations between $\mathbf{A}^{+}$ and $\mathbf{A}^{-}$ the six quantities f^{+}, f^{-} are not independent. Three scalar integrations suffice to determine the two for a given set of indices, whereas one might suppose two vector integrations to be needed.

It is to be emphasized that the above formula is extremely simple to compute with because of the extreme rapidity of convergence. This arises because with increasing n the functions vanish more and more rapidly at the origin so that very few terms are needed. In practice it is found that the radiation resistance of most antennae can be found with a very small amount of labor.

We note that to get the total radiation it is not necessary to compute the fields. In fact, it is rather harder actually to compute the fields than to find the total radiation. It is plain that we can, if we wish, easily separate the energy which is eventually absorbed in the ground from that which is radiated upward.

This completes the treatment of the problem of computing the total radiation. The functions introduced above may also be made the basis of two interesting expansions which we now give. In deriving these expansions we note that when there is no ground the expression (8) for the vector potential is particularly simple and that $\boldsymbol{A}$ is also given by $(1/4\pi c)\int \mathbf{i}(e^{ikr_{12}}/r_{12})d\tau$. Identifying these expressions for arbitrary values of $\mathbf{i}$ leads to a vector expansion of the type found in the first reference:

$$\mathbf{i}(1)\frac{e^{ikr_{12}}}{r_{12}}=i\sum_n\int_0^\infty\left[\frac{l}{k^2}\mathbf{A}^+_{1,\,n}(2)\mathbf{i}(1)\cdot\bar{\mathbf{A}}^+_{1,\,-n}(1)+\frac{1}{l}\mathbf{A}^+_{2,\,n}(2)\mathbf{i}(1)\cdot\bar{\mathbf{A}}^+_{2,\,-n}(1)+\frac{1}{l}\mathbf{A}^+_{3,\,n}(2)\mathbf{i}(1)\cdot\bar{\mathbf{A}}^+_{3,\,-n}(1)\right]\frac{dl}{m},\quad z_1>z_2. \tag{12}$$

Here r_{12} is the distance between the two points whose coordinates are denoted by 1 and 2.

There is another expansion of this general type possible in cylindrical coordinates. Let $\mathbf{A}_1'$, $\mathbf{A}_2'$, $\mathbf{A}_3'$ be three vectors generated in the manner prescribed by (1) but with the Bessel function in ξ replaced by a Hankel function of the first kind. Also let us delete the superscript $\pm$ from the $\mathbf{A}$'s of (1) and consider m as running from $-\infty$ to $+\infty$.

Then we use methods like those above, but divide the current into thin cylindrical shells instead of into laminae. In this way we find

$$\mathbf{i}(1)\frac{e^{ikr_{12}}}{r_{12}}=\frac{i}{2}\sum_n\int_{-\infty}^{+\infty}\left[\frac{1}{k^2}\mathbf{A}'_{1,\,n}(2)\bar{\mathbf{A}}_{1,\,n}(1)\cdot\mathbf{i}(1)+\frac{1}{l^2}\mathbf{A}'_{2,\,n}(2)\bar{\mathbf{A}}_{2,\,n}(1)\cdot\mathbf{i}(1)+\frac{1}{l^2}\mathbf{A}'_{3,\,n}(2)\bar{\mathbf{A}}_{3,\,n}(1)\cdot\mathbf{i}(1)\right]dm,\quad r_2>r_1. \tag{13}$$

This expansion (13) is in the same relation to (12) above as are (12) and (13) of the second reference. Using (13) to find the fields and then the integral of the Poynting vector in the same manner as above, one is led to an expression that is identical with (11) with the α's equal to zero.

Using the above formulae we have computed the radiation from a number of typical antennae. We hope to publish this soon in the *Proceedings of the Institute of Radio Engineers*.

Cathode Sputtering in Arc Discharges

LEWIS R. KOLLER, *Research Laboratory, General Electric Company, Schenectady, N. Y.*

(Received April 9, 1936)

A method is described for measuring the number of atoms of thorium sputtered from tungsten by positive ions of various velocities in the positive column of an arc discharge. The threshold for mercury ions is 35 volts. The number of atoms sputtered per positive ion in mercury vapor increases with increase in filament temperature and with decrease in arc current. The effectiveness of ions in sputtering thorium from tungsten is in the order neon, argon, mercury. Measurements of emission from a probe permit observations of the rate of loss of barium from an oxide coated cathode. The threshold for sputtering from a cold oxide coated filament by neon ions is approximately 45 volts. The material sputtered is not electrically charged. There is a difference in nature between the material evaporated and sputtered from an oxide coated cathode. The threshold for sputtering of barium from tungsten is 14 volts for argon ions and approximately the same for neon. The arc current to a coated cathode reduces the rate of loss of coating material under certain conditions.

I. The Sputtering of Thorium from Tungsten by Mercury Ions

MEASUREMENTS of cathode sputtering have been made by a large number of observers. Those up to 1927 have been summarized by Fischer.[1] All of the earlier measurements, and all but three of the more recent ones were made at high voltages. The measurements by Kingdon and Langmuir,[2] by Hull[3] and by Luder[4] were made at voltages below 100 volts. It is this low voltage range which is of particular interest in the operation of hot cathode discharge tubes.

The following measurements of the sputtering of thorium by mercury were made by a modification of the method of Kingdon and Langmuir. Positive ions from an arc discharge were allowed to bombard a thoriated tungsten filament. The amount of material sputtered was determined from measurements of thermionic emission from the filament. The ion currents and ion velocity were determined by probe measurements. This method differs from that of Kingdon and Langmuir in that it is possible to obtain much larger positive ion currents and so carry the measurements more easily into the range where there is little sputtering. Its disadvantage is that the thermionic currents cannot readily be measured with the same degree of accuracy in high pressures of gas as in low pressures.

A positive column tube of the form shown in Fig. 1 was used. The distance between cathode and anode was 16 inches and the tube diameter was 2 inches. The main cathode, C, was an oxide-coated filament. An arc discharge of from 0.06 to 1.5 amperes was passed from this cathode to the anode, A. The tube drop was approximately 35 volts. The filament studied, F, was thoriated tungsten 0.006 inch $\times$ 2 inches wound in the form of a helix $\frac{1}{4}$ inch in diameter, and placed in the positive column at a distance of 6 inches from the anode. The filament leads were covered with glass insulators. The mercury vapor was supplied by a few drops of mercury distilled into the tube at the end of exhaust. The residual gas pressure was sufficiently low, so that the filament emission was not substantially affected by letting the tube stand cold overnight.

By making the filament negative with respect to the discharge it could be bombarded with positive ions. Under these conditions a positive ion sheath was formed around the filament, and the ions acquired all their velocity in falling through this sheath. Accordingly, in order to know the drop in the sheath, it was necessary to determine the space potential. The space potential was determined by means of a probe filament, P, of tungsten 0.007 inch $\times \frac{3}{8}$ inch opposite the thoriated filament and similarly situated in the

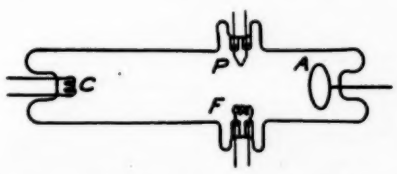

FIG. 1. Positive column discharge tube.

[1] Fischer, Fortschritte d. Chemie Physik und Physik. Chemie **19**, 1 (1927).
[2] Kingdon and Langmuir, Phys. Rev. **22**, 148 (1923).
[3] A. W. Hull, Trans. Am. Inst. Elec. Eng. **47**, 775 (1928).
[4] H. Luder, Zeits. f. Physik **97**, 158 (1935).

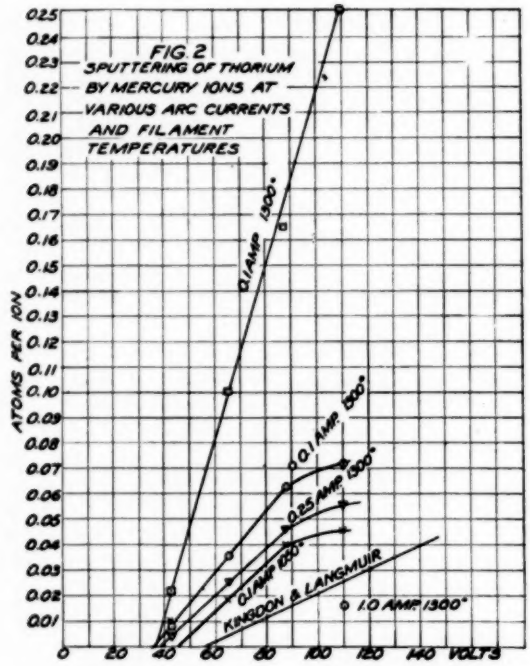

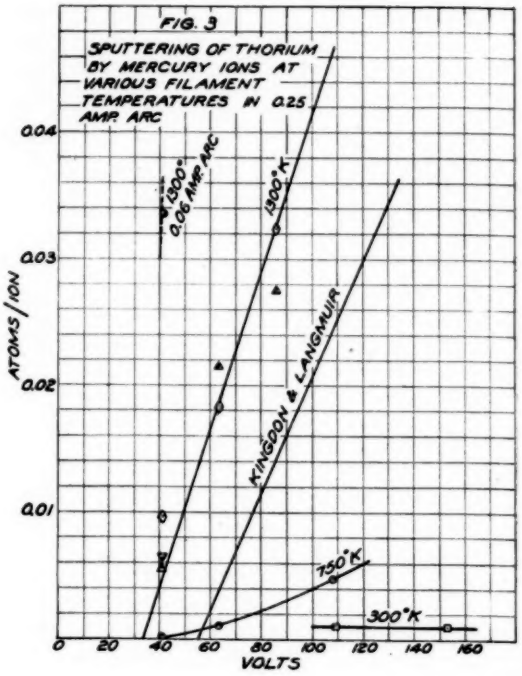

tube. The potential of this probe was varied from -165 to -6 volts with respect to the anode, and space potential was determined from a semilogarithmic plot of the probe volt-ampere characteristic. It was found to be -12 volts with respect to the anode.

The method of measuring thermionic emission in gases has been described by Found.[5] In measuring emission the filament was heated to a temperature of 1725°K, and the current from it measured at -30 volts with respect to the anode. The positive ion current to the cold filament was subtracted from this value. Under the testing conditions the filament accordingly was at a potential of -18 volts with respect to the plasma. The temperature of the filament was then lowered, and its negative potential with respect to the plasma was raised to the desired sputtering value for a convenient time interval. The time interval used was from 0.5 to 30 sec. and was determined by a commutator. The filament temperature was lowered 30 sec. before sputtering, in order to allow time for cooling. The mercury vapor pressure corresponded to room temperature, approximately 25°C. The fraction of the surface covered was calculated from a log $i \sim \theta$ curve.[6] No correction was made for lead losses. The procedure then consisted in first measuring emission, then sputtering for a time interval sufficient to reduce θ by about 0.02 to 0.15θ, and finally measuring the emission again. From the value of $-\Delta\theta$, the positive ion current and time of sputtering, the number of thorium atoms removed per Hg ion was calculated. The results of a large number of measurements at different values of filament temperature and arc current are shown in Fig. 2. The arc current and the filament temperature are indicated on each curve. Each point shown is the average of from 2 to 4 readings. From the figure it can be seen that up to about 100 volts the number of atoms sputtered per ion is proportional to the ion velocity. At higher voltages it increases less rapidly than the voltage. It decreases with increasing arc current and with decreasing filament temperature. The curves indicate a threshold in the neighborhood of 35 volts.

The effect of the arc current on the number of atoms sputtered per positive ion is difficult to interpret. At high values of vapor pressures, high sputtering voltage and small arc currents, the mean free path of the ions becomes small compared with the thickness of the ion sheath. Under these conditions the ions may make several collisions within the sheath before striking

[5] C. G. Found, Phys. Rev. **45**, 519 (1934).
[6] I. Langmuir, J. Frank. Inst. **217**, 543 (1934).

the filament. Thus they lose energy and their velocity may be very much less than that corresponding to the drop in the sheath. This gives a spuriously low rate of sputtering. For example, in Hg vapor the values of sheath thickness, mean free path and rate of sputtering for 120 volt ions for two different bulb temperatures are shown below.

T°C	Sheath thickness	λ	Atoms/ion
27	1.59 mm	11.3 mm	0.037
75	0.9	0.38	0.0167

At the higher pressure the sheath thickness is large compared with the mean free path, and the number of atoms sputtered per ion is half of the normal value. At room temperature, however, the sheath thickness is of the order of 0.1λ for the arc currents studied so that this effect should not be observed. Furthermore, since the diameter of the sheath increases as the arc current decreases one would expect just the reverse effect.

The most probable explanation for the effect of filament temperature is that a film of Hg condenses on the surface of the filament and that the Hg atoms must be sputtered off before there can be any sputtering of Th. At low temperatures the filament is completely covered with Hg while at higher temperatures it is only partially covered, so that the rate of sputtering of thorium is higher. It is not possible to test this theory by varying the vapor pressure within wide limits on account of the effect on the sheath diameter. Fig. 3 shows a set of measurements made at filament temperatures of 300°K, 750°K and 1300°K under the same arc conditions. At 300° the rate of sputtering was so low that accurate measurements could not be made for ion velocities below 100 volts. At 100 volts the rate of sputtering from a filament at 1300° is 10 times as great as from one at 750°K.

Some qualitative measurements made in a similar tube in argon showed that the rate of sputtering was of the same order of magnitude as for mercury, and that there was little if any effect of filament temperature. The ratio between the rate at 1300° and at 25° was not greater than 2, whereas in mercury it was 40. This would support the view that the temperature effect is due to a film condensed on the filament surface.

The apparent effect of sheath thickness is shown for two different pressures of argon in the following table.

P	Ion vel.	Arc amps.	Sheath thickness	λ	Atoms/ion
60 μ	75	2.0	0.19	0.12 mm	0.01
2 mm	120	1.5	0.53	0.036 mm	0.0014

If we assume the same threshold for argon as for mercury, the rate of sputtering for 75 volt-ions in the 2-mm arc would be $40/85 \times 0.0014 = 0.00066$ atom per ion. Thus the rate of sputtering in the low pressure arc where the sheath and mean free path are comparable is 16 times as great as the apparent rate when the mean free path is small compared with the sheath.

Measurements of emission in argon were unreliable due to the exponential relation[7] between thermionic emission and current to the filament as well as high secondary emission from the filament.

In addition to using this method for quantitative measurements of rate of sputtering, once the rate has been determined it should be possible to place thoriated filaments at various points in the discharge and use the rate of sputtering as a measure of space potential.

Some preliminary measurements which preceded those which have just been described were made in cathodic tubes of the type shown in Fig. 4. The results are shown in Fig. 5. At the time that these measurements were made the effect of the filament temperature was not known. The procedure was to open the filament circuit before sputtering, but the time between opening the circuit and commencing to sputter was not carefully controlled. Accordingly, the temperature of the filament varied from reading to reading, depending upon chance variations in this time interval. Except for the case of mercury this probably does not affect the results greatly. The results are less reliable than those taken in the positive column, because of the uncertainty of the probe method of determining space potential in the cathodic discharge, and because of the short filament used. They are presented here for the comparison of sputtering in argon and neon. The neon shows a much higher rate than the argon at the same voltage, and a threshold of 33 volts as compared with 45 for

[7] K. Blodgett, Proc. Nat. Acad. Sci. **15**, 233 (1929).

argon. The absolute values are not in agreement with those made in the positive column.

II. The Sputtering of Oxide-Coated Cathodes

Measurements of the sputtering of oxide-coated cathodes were made by a modification of the method used for thorium. Observations of sputtering cannot be made by emission measurements directly on heavily coated cathodes since after a period of bombardment they reactivate during the course of an emission reading. Accordingly, the procedure was modified by studying the behavior of a tungsten filament placed in the discharge. Barium from the discharge deposited on this filament, and its emission was then used as an indication of phenomena taking place at the main cathode.

The following measurements were made in a cathodic tube similar to that shown in Fig. 4. A large tungsten helix and an oxide-coated cathode were placed on opposite sides of an 0.007 inch $\times 1$ inch tungsten filament which was in the axis of a $1\frac{1}{2}$ inch $\times 1\frac{1}{2}$ inch cylindrical nickel anode in 2 mm of neon. A 0.1-ampere arc was passed between the tungsten helix and the anode. The emission from the straight tungsten filament could then be measured by the method already described. This filament will be referred to hereafter as the probe.

The cold coated cathode was made negative with respect to the plasma and bombarded by a positive ion current of from 5 to 10 milliamperes. Material sputtered from this cathode deposited on the straight probe. This was heated by a current of 1.75 amperes and maintained at a potential of -6 volts with respect to the anode. The time required for the emission from this probe to reach a maximum was measured for different values of sputtering voltage applied to the coated cathode. It was assumed that the same state of activation indicated the same amount of barium collected on the surface of this probe, and therefore the same amount sputtered from the coated cathode. The reciprocal of this time is proportional to the rate of sputtering. The reciprocals of time calculated for equal positive ion currents are plotted against voltage in Fig. 6. The extrapolated curve shows a threshold for sputtering from a cold oxide-coated cathode of about 56 volts. Definite sputtering, however, was observed at 45 volts. It is possible that the curve "tails off" in the neighborhood of the threshold.

In a similar tube in 600μ neon the potential of the collecting probe was varied from -6 to $+12$ volts with respect to the anode. There was no significant difference between the amounts of active material collected at these voltages in equal intervals of time, indicating that the sputtered material is not charged.

There is a marked difference in the character of the material removed from an oxide-coated cathode by sputtering and by evaporation. A cathodic tube of the type described above was used filled with 600μ of neon. The emission measurements were made with a heater current of 1.5 amperes through the probe filament while it was at a potential of -6 volts with respect to the anode. The probe was only heated during the time that emission measurements were being made. While barium was being collected it was at a potential of -6 volts with no heater current passing through it.

In the first series of experiments the arc current was kept constant, and a constant heater current was passed through the oxide-coated cathode. Material evaporated from it and deposited on the probe. The probe was flashed at a high temperature to clean the surface before each

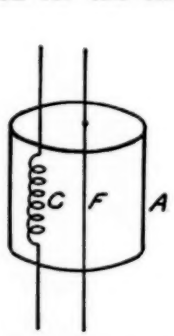

Fig. 4. Cathode discharge tube. *A*, cylindrical anode $1\frac{1}{2}'' \times 1\frac{1}{2}''$; *C*, tungsten cathode; *F*, thoriated filament.

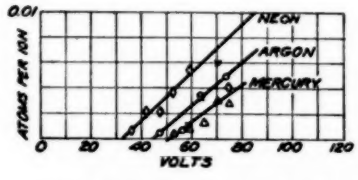

Fig. 5. Sputtering of thorium in cathodic discharge in various gases.

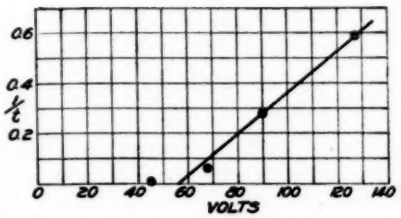

FIG. 6. Rate of sputtering of cold coated cathode in 2-mm neon.

run, and its heater current then turned off. After a definite time interval the heater current of the coated cathode was turned off, and the emission from the probe was measured. The probe emission decreased rapidly due to evaporation from its surface. The deactivation curves of the probe after having collected barium for various time intervals are shown in Fig. 7. After collecting barium for $1\frac{1}{4}$ min., the initial emission was low, and the rate of deactivation high. A collecting period of two minutes gave a much higher initial emission, but the probe still began to deactivate immediately on heating. A nine minute collecting period did not give any higher initial emission than a two minute period, indicating that the latter was sufficient to give a surface completely covered with a monatomic barium layer. Covering the surface with a polyatomic layer did not change the rate of deactivation appreciably, since the additional layers evaporate almost instantaneously upon heating.

A deposit of an entirely different character was obtained by sputtering. In this case the oxide-coated cathode was not heated. After flashing the probe the coated cathode was made 120 volts negative with respect to the anode for various time intervals. The ion current to it was 3×10^{-3} ampere. The sputtering circuit was then opened, and the emission from the probe filament measured. In this case the probe activated during the course of the emission measurements, passed through a maximum and deactivated. A series of these deactivation curves for different initial collecting periods is shown in Fig. 8. Initial sputtering periods of 5 and 10 seconds are not enough to give a completely covered surface. After a fifteen-second period the maximum emission of 20×10^{-3} ampere is reached. Increasing the sputtering period, which presumably increases the thickness of the deposit on the probe, increases the time required to reach the maximum and decreases the rate of deactivation. A 5-minute sputtering period results in a very flat maximum. The difference in the character of the evaporated and sputtered deposits is probably due to the fact that evaporation is a selective process and that the material evaporated from the coated cathode is largely barium, while the sputtered material is barium plus barium oxide. The former has a much higher rate of reevaporation from the probe than the latter. The activation of the sputtered deposit is a reorientation phenomenon. If the evaporation from the coated cathode is carried out at a higher temperature, a deposit is obtained which behaves in a manner similar to the sputtered deposit. This is shown in Fig. 9. This deposit was formed by heating the coated cathode at 13 amperes instead of its normal current of 10 amperes. The probe filament shows an initial activation, and no appreciable evaporation over the 10-minute observation period. At the higher temperature barium oxide evaporates from the cathode as well as barium, and forms a deposit similar in behavior to the sputtered one.

In another tube in 600μ of argon no difference was observed between the sputtered and evaporated deposits. The shape of these activation curves must of course depend on the previous history of the cathode which is acting as a source of barium. The behavior of a probe may be a more fruitful method of studying cathodes than by making direct measurements of the cathodes themselves.

Because of the difficulty in making sputtering measurements directly on a coated cathode, the sputtering from a probe coated by evaporation was investigated. A probe coated by evaporation deactivates rapidly at the temperatures required to make thermionic emission measurements. Low testing temperatures cannot be used since under these conditions the electron currents are small compared with convenient values of ion currents. Accordingly, it was decided to keep the probe activated by continuously evaporating barium onto it from the coated cathode. Under these conditions the probe emission would reach an equilibrium value determined by the rate of supply of barium to it from the cathode and the rate of loss of barium from it by evaporation and sputtering.

The experiments were performed in a cathodic tube of the type of Fig. 4 in 1 mm of argon. A 0.1-ampere arc was passed to the tungsten helix. The coated cathode was operated at 10.5 amperes continuously and the probe was held at 1.75 amperes. The potential of the probe with respect to the anode was varied and its emission was measured. The results are shown in Fig. 10 where the emission readings are plotted against time. At -6 volts the probe activated rapidly reaching a steady state in 2 min. Its potential was then raised to -12 volts. The emission current increased initially due to the increased ionization by the thermionic electrons and then decreased to a new equilibrium value. The drop in emission was due to sputtering which increased the rate of loss from the probe. The probe potential was then increased in 2-volt steps to -16 volts, each voltage resulting in a new and lower equilibrium value of emission due to increased sputtering. The positive ion current was nearly independent of voltage being 0.8×10^{-3} ampere at -6 volts, and 1.1×10^{-3} ampere at -18 volts. From the figure it can be seen that some sputtering takes place at -12 volts. The space potential was $+2$ volts. Accordingly, the threshold for sputtering of barium from a hot tungsten filament by argon ions lies below 14 volts. An estimate of the rate of sputtering at 18 volts gave 5×10^{-4} atom per ion. A similar experiment in neon gave a threshold of less than 15 volts.

Although no evidence has been found to show that barium which finds its way into an arc is charged, in a great many cases the loss of barium from the cathode appears to be affected by the arc in a manner which cannot be accounted for by temperature alone. For example, in the tube just described the rate of activation of the probe was measured when the coated cathode was run at constant current, first with no arc current and secondly with an arc current of 0.1 ampere. The probe reached the same state of activation in 7 and 30 minutes, respectively. Accordingly, the 0.1-ampere arc current reduced the rate of loss of barium from the coated cathode to $\frac{1}{4}$ of the zero arc rate. The cooling effect of 0.1 ampere of electron current, even assuming a work function as high as 3 volts, would only amount to 0.3 watt which would be negligible in comparison with the input to the filament which was 20 watts. Effects of this kind have been very inconsistent, and the phenomena may depend on the surface condition of the filament.

Another series of experiments under slightly different conditions was performed in a cathodic discharge in 2 mm of argon. The coated cathode

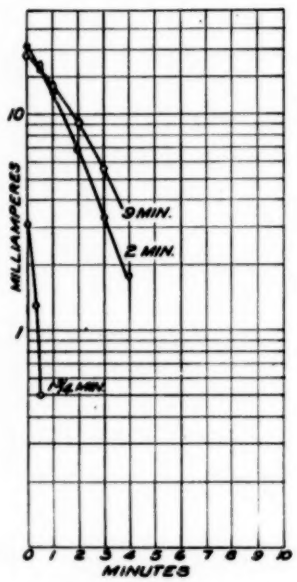

FIG. 7. Evaporation of evaporated deposit from probe.

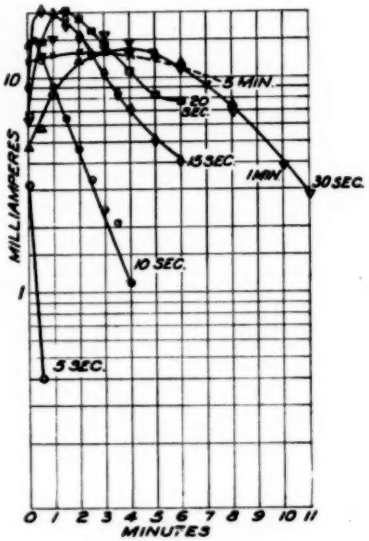

FIG. 8. Evaporation of sputtered deposit from probe.

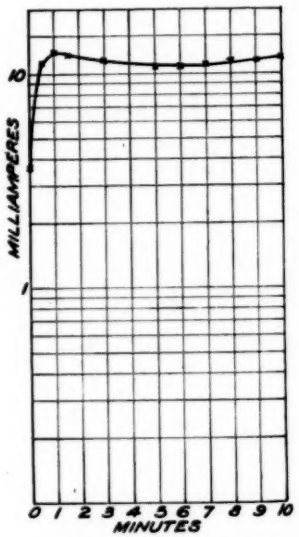

FIG. 9. Evaporation from probe of deposit formed by high temperature evaporation.

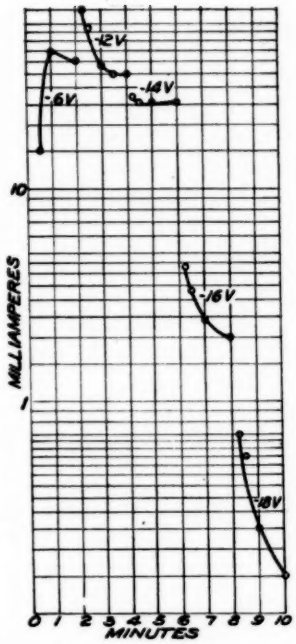

FIG. 10. Sputtering of Ba from W in 1 mm-argon.

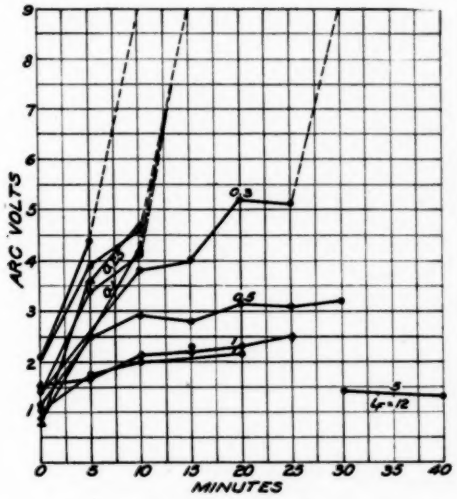

FIG. 11. Life of evaporated deposits on tungsten filament at various arc currents in 2-mm argon.

was first flashed at 150 percent of normal current for 2 min. This caused the evaporation of sufficient barium to coat the tungsten helix. The coated cathode heater circuit was opened, the tungsten helix was heated at 1687°K, and a one-ampere arc operated between it and the anode. The initial value of arc drop was 1.55 volts which increased in 25 minutes to 2.5 volts. In another case the arc operated at one ampere for over 87 minutes and at five amperes for 40 minutes, when the run was discontinued. At 40 minutes the drop was 3.5 volts. The filament was then flashed to clean the surface and reactivated by heating the coated cathode and a 0.5-ampere arc operated. This was discontinued after 30 minutes. This arc drop, as can be seen from Fig. 11, reached a value of 3.2 volts in 30 minutes. The filament was then reactivated as before and runs were made at 0.3, 0.25, 0.1 ampere. The 0.3-ampere arc reached a voltage of 5.1 in 25 minutes and then went out. The 0.25 and 0.1-ampere arcs went out at the end of 10 minutes. When the filament was simply heated with no arc current, the arc could not be struck after 15 minutes. Thus in order to maintain the active coating on the filament, it is necessary to draw an arc current of about one ampere. The wattage input to the filament was 27 watts. Here again the cooling effect of the electron current does not seem to be sufficient to account for the observed phenomena. The observed arc drop which was measured by a d.c. meter to the mid tap of the filament transformer should be increased by the peak value of filament drop 2.13 volts. Even with this correction the drop is only 3.68 volts. This low drop is a characteristic of tungsten cathodes coated by evaporation. The arc drop was always lower to the evaporation cathode than it was to the coated cathode of the same shape and size in the same tube.

The experiment was repeated in a similar tube at a pressure of 600μ of argon. The results were inconsistent and not conclusive. No effect was observed in 2 mm of neon. The rate of sputtering in neon is probably very high compared with any mechanism tending to return barium to the cathode. No effect was observed in 2 mm of helium.

In similar tubes in mercury an evaporated cathode was operated with a one ampere arc for as long as four hours with the tube at a bulb temperature of 85–89°C. The arc drop increased from a value of 2.7 volts 40 minutes after starting to 5.7 volts 15 minutes before the arc went out. At 65° the arc only ran for 10 minutes while at 53° it went out immediately on starting. Another tube operated at 48° but would not operate at 36°. This effect is probably one of sputtering since at the lower values of pressure the arc drop is above the threshold for sputtering.

A Heat Transfer Problem of Interest in Calorimetry

JULIAN M. STURTEVANT, *Yale University*

(Received April 2, 1936)

A boundary value problem which may be applied to certain cases of heat transfer is worked out. The solution is applied to the investigation of the lags occurring in a medium of finite thermal conductivity enclosed in an infinitely long cylindrical case of infinite thermal conductivity when heat is introduced uniformly into the case, and when heat is evolved uniformly within the medium.

IN connection with the development of a calorimetric method for determining the rates of chemical reactions it became necessary to investigate the magnitude of the temperature lags occurring in a cylinder of liquid contained in an electrically heated platinum case, the heat capacity of the case not being negligible. This calculation involved a boundary value problem to which other cases of heat transfer can be referred. In the present report the mathematical problem will first be worked out and then applied to two cases of heat transfer.

Boundary Value Problem

Consider a function $y(r, t)$ which satisfies the differential equation

$$\frac{1}{r}\frac{\partial}{\partial r}\left(r\frac{\partial y}{\partial r}\right)=\gamma\frac{\partial y}{\partial t}, \quad 0\leq r\leq 1, \quad 0\leq t<\infty \tag{1}$$

and which must be fitted to the boundary conditions

$$m\left(\frac{\partial y}{\partial r}\right)_{r=1}+n\left(\frac{\partial y}{\partial t}\right)_{r=1}=k, \quad k=\text{a constant} \tag{2}$$

and

$$y(r, 0)=f(r). \tag{3}$$

A general solution of this problem can be obtained in the form

$$y(r, t)=z(r, t)+z_1(r, t), \tag{4}$$

where $z(r, t)$ is the general solution of the corresponding homogeneous problem with $k=0$ and Eq. (3) replaced by

$$z(r, 0)=f(r)-z_1(r, 0) \tag{5}$$

and $z_1(r, t)$ is a particular solution satisfying Eqs. (1) and (2) but not (3). It is easily verified that

$$z_1(r, t)=\frac{2kt}{m\gamma+2n}+\frac{k\gamma r^2}{2(m\gamma+2n)} \tag{6}$$

satisfies these conditions. Thus we must determine $z(r, t)$ so that

$$z(r, 0)=f(r)-\frac{k\gamma r^2}{2(m\gamma+2n)}. \tag{7}$$

Homogeneous Problem

Separation of Eq. (1) in the usual way leads to the particular solution

$$z=\exp(-\alpha^2 t/\gamma)J_0(\alpha r), \tag{8}$$

where J_0 is the Bessel function of the first kind and zero order. On substitution in Eq. (2) (with $k=0$) it is found that the separation constant α must be a root of

$$F(\alpha)=\lambda\alpha J_0(\alpha)+J_1(\alpha), \qquad \lambda=n/m\gamma. \tag{9}$$

It seems safe to assume without proof that the roots of $F(\alpha)$ are all real and distinct, with the possible exception of the root $\alpha=0$, which may be multiple. At any rate it will be assumed that an arbitrary continuous single-valued function, say $z(r, 0)$, can be expressed in the form

$$z(r, 0)=\sum_{i=0}^{\infty}A_i J_0(\alpha_i r), \tag{10}$$

where the α_i are the successive *positive* roots of $F(\alpha)$, $\alpha_0=0<\alpha_1<\alpha_2\cdots$. The function $F(\alpha)$ is an odd function, so for each real positive root there will be a negative root of equal magnitude. It is thus only necessary to sum over the positive roots since $J_0(\alpha_i r)$ is an even function.

The general solution of the homogeneous problem is taken in the form

$$z(r,t)=\sum_{i=0}^{\infty}A_i \exp(-\alpha_i^2 t/\gamma)J_0(\alpha_i r), \quad (11)$$

where the A_i are evidently identical with the A_i in Eq. (10). In determining the A_i it must be noted that the functions $J_0(\alpha_i r)$ are orthogonal in a generalized sense, since

$$\int_0^1 J_0(\alpha_i r)J_0(\alpha_j r)r\,dr$$

$$=[\alpha_i J_0(\alpha_j)J_1(\alpha_i)-\alpha_j J_0(\alpha_i)J_1(\alpha_j)]/(\alpha_i^2-\alpha_j^2)\neq 0, \quad i\neq j,$$

a relation which follows from the well-known properties of the Bessel functions. On using the fact that α_i and α_j are roots of $F(\alpha)$ it is found that

$$\int_0^1 J_0(\alpha_i r)J_0(\alpha_j r)r\,dr+\frac{n}{m\gamma}J_0(\alpha_i)J_0(\alpha_j)=0, \quad i\neq j, \quad (12)$$

The corresponding normalization relation is found to be

$$\int_0^1 [J_0(\alpha_i r)]^2 r\,dr+\frac{n}{m\gamma}[J_0(\alpha_i)]^2$$

$$=\left(\frac{1}{2}+\frac{n}{m\gamma}+\frac{n^2\alpha_i^2}{2m^2\gamma^2}\right)[J_0(\alpha_i)]^2. \quad (13)$$

To evaluate the coefficients A_i we multiply each side of Eq. (10) by $J_0(\alpha_j r)r\,dr$ and integrate from 0 to 1; to the resulting equation we add the identity

$$\frac{n}{m\gamma}z(1,0)J_0(\alpha_j)=\frac{n}{m\gamma}\sum_{i=0}^{\infty}A_i J_0(\alpha_i)J_0(\alpha_j).$$

After taking account of Eqs. (12) and (13) we obtain

$$A_i=\frac{\int_0^1 z(r,0)J_0(\alpha_i r)r\,dr+(n/m\gamma)z(1,0)J_0(\alpha_i)}{(1/2+n/m\gamma+n^2\alpha_i^2/2m^2\gamma^2)[J_0(\alpha_i)]^2}. \quad (14)$$

The integral in this expression can be evaluated when the form of $z(r,0)$ has been determined in any particular application.

Determination of the α_i

The roots of the function $F(\alpha)$ can be readily calculated for the cases $\lambda\ll 1$ and $\lambda\gg 1$. For $z=\alpha_i$

$$-\lambda=J_1(z)/zJ_0(z);$$

then, if we consider z as a function of λ, we have[1]

$$\frac{dz}{d\lambda}=\frac{-z}{1+2\lambda+z^2\lambda^2}.$$

Expanding $z(\lambda)$ by Taylor's theorem about the point $\lambda=0$ we obtain

$$\alpha_i=\zeta_i-\zeta_i\lambda+\frac{3}{2}\zeta_i\lambda^2+\frac{2\zeta_i^3-15\zeta_i}{6}\lambda^3$$

$$-\frac{44\zeta_i^3-105\zeta_i}{24}\lambda^4+\cdots, \quad (15)$$

where ζ_i is a root[2] of $J_1(z)$.

Similarly, if $\lambda\ll 1$ we find that

$$\alpha_i=\xi_i+\frac{1}{\xi_i}\frac{1}{\lambda}-\frac{3}{2\xi_i^3}\frac{1}{\lambda^2}+\frac{25-2\xi_i^2}{6\xi_i^5}\frac{1}{\lambda^3}$$

$$-\frac{343-44\xi_i^2}{24\xi_i^7}\frac{1}{\lambda^4}+\cdots, \quad (16)$$

where ξ_i is a root of $J_0(z)$. It is to be noted that Eq. (16) converges rapidly for $\lambda\approx 1$ and $i>2$ since ξ_i is then large.

Another expression for these roots which is useful in some cases may be obtained by application of Stokes' method[3] for calculating the roots of $J_n(z)$. The result is

$$\frac{\alpha_i}{\pi}=i-\frac{1}{4}+\frac{8+\lambda}{2\pi^2\lambda(4i-1)}$$

$$-\frac{128+576\lambda+48\lambda^2+31\lambda^3}{6\pi^4\lambda^3(4i-1)^3}+\cdots. \quad (17)$$

This expression will only be useful for fairly large values of i and λ not much less than unity.

---

[1] Whittaker and Watson, *Modern Analysis*, third edition, p. 380, example 14.

[2] Extensive tables of J_0 and J_1, including their roots, are given by Jahnke and Emde, *Funktionentafeln*, second edition, p. 228.

[3] See Gray, Mathews and MacRoberts, *Bessel Functions*, p. 86.

Applications

Case I

An infinitely long cylindrical metal case contains a liquid (or other material) of finite thermal conductivity. Heat is introduced into the metal case uniformly (from an electrical resistance winding on the case, for example) and at a constant rate. The initial temperature is constant throughout the system. The temperature difference between the metal case and its surroundings is kept constant (by adjustment of the temperature of the surroundings). Heat transfer due to convection in the liquid is neglected. C.g.s. units are used throughout.

Let

k = thermal conductivity of the liquid,
c = specific heat of the liquid,
ρ = density of the liquid,
K = heat capacity of the metal case per centimeter,
Q = rate of heat input into the metal case in calories per second per centimeter,
T_0 = initial temperature of the cylinder and contents,
T' = constant temperature difference between the cylinder and surroundings,
e = emissivity of the metal case,
R = inside radius of the case.

The thermal conductivity of the metal case is assumed to be infinite.

The fundamental equation for this problem is the Fourier conduction equation

$$\frac{1}{r}\frac{\partial}{\partial r}\left(r\frac{\partial T}{\partial r}\right)=\frac{c\rho}{k}\frac{\partial T}{\partial t}, \quad 0\leq r\leq R.$$

The boundary conditions are

$$Q-2\pi kR\left(\frac{\partial T}{\partial r}\right)_{r=R}=eT'+K\left(\frac{\partial T}{\partial t}\right)_{r=R},$$

$$T(r,0)=T_0.$$

The substitution $x=r/R$ changes this to the problem solved above. In carrying out the calculations it is necessary to use the relation

$$\int_0^1 J_0(\alpha r)r^3dr=\frac{1}{\alpha^2}\left(2+\frac{4n}{m\gamma}-\frac{n\alpha^2}{m\gamma}\right)J_0(\alpha), \quad \alpha\neq 0,$$

obtained by direct integration and use of the fact that α is a root of $F(\alpha)$. The final result is

$$\frac{T(r,t)-T_0}{Q'}=\frac{1}{\pi k(1+2\lambda)}\left[\tau+\frac{\pi c\rho r^2\lambda}{2K}-\sum_{n=0}^{\infty}c_n e^{-\alpha_n^2\tau}J_0\left(\alpha_n\frac{r}{R}\right)\right], \quad (18)$$

where

$$c_0=\frac{1+4\lambda}{8(1+2\lambda)}, \quad c_n^{-1}=\left(1+\frac{\alpha_n^2\lambda^2}{1+2\lambda}\right)\alpha_n^2J_0(\alpha_n),$$

$$Q'=Q-eT', \qquad \tau=\frac{2\pi k\lambda}{K}t,$$

and the α_n are the roots of $F(\alpha)$ with

$$\lambda=K/2\pi c\rho R^2.$$

To facilitate use of this result a set of values of the α_n for various values of the parameter has been calculated. These values are given in Table I, in a form which renders interpolation more accurate. The tables in Jahnke and Emde[2] were used in these calculations.

As might have been expected, Eq. (18) shows that the time lags are independent of the rate of heating. It should be observed that any convection will serve to decrease the radial lags, though vertical lags will of course be introduced. However with a cylinder of liquid of sufficiently small radius convection should not seriously invalidate Eq. (18).

TABLE I. *Values of* $(\alpha_n-\xi_n)$ *for various values of* λ *and* $\eta\cdot\xi_n=a$ *root of* $J_0(\alpha)$.

λ \ n	1	2	3	4	5	6
0.0	1.427	1.496	1.520	1.532	1.540	1.545
0.1	1.104	0.943	0.786	0.661	0.564	....
0.2	0.885	.650	.488	.383	.314	....
0.3	.734	.488	.348	.266	.215	....
0.4	.625	.388	.269	.203	.163	....
0.5	.545	.321	.219	.164	.131	....
0.6	.482	.274	.185	.138	.110	....
0.7	.432	.238	.159	.119	.094	....
0.8	.392	.211	.140	.104	.083	....
0.9	.358	.189	.125	.092	.074	....
1.0	.330	.171	.113	.083	.067	0.055
2.0	.184	.088	.057	.042	.034	.028
3.0	.127	.059	.039	.028	.022	.018
4.0	.097	.044	.029	.021	.017	.014
5.0	.079	.036	.023	.017	.013	.011
6.0	.066	.030	.019	.014	.011	.009
7.0	.057	.026	.017	.012	.010	.008
8.0	.050	.023	.014	.011	.008	.007
9.0	.045	.020	.013	.009	.007	.006
10.0	.041	.018	.012	.008	.007	.006
ξ_n	2.405	5.520	8.654	11.792	14.931	18.071

It is of interest to investigate the time which must pass before the temperature everywhere in the cylinder will rise linearly with the time. To do this we calculate the minimum value of the time for which the first exponential term is less than one percent of the preceding terms for $r=0$. We therefore wish to find the minimum value of τ for which

$$100e^{-\alpha_1^2\tau_{\min}} \leq |c_1^{-1}|\left[\tau_{\min}-\frac{1+4\lambda}{8(1+2\lambda)}\right].$$

The values of $\tau_{\min}$ obtained in this way are given in Table II. It is evident that the heat capacity of the system could be determined after this time by measuring the temperature increase, at any convenient point, corresponding to a known heat input, provided the rate of heat input is kept constant.

TABLE II. *Values of time* ($t_{\min}=K\tau_{\min}/2\pi k\lambda$) *after which temperature rises linearly with time.*

λ	0.0	0.1	0.2	0.5	1.0	2.0	3.0	6.0	8.0	10.0
$\tau_{\min}$	0.308	0.364	0.409	0.494	0.564	0.622	0.647	0.676	0.684	0.686

Case II

This case is very similar to the one described above, the only difference being that a quantity of heat, Q calories, is evolved per second per cubic centimeter in the liquid, and no heat is introduced into the metal case from outside. The solution of this case will be a first approximation to the more complicated case of a decreasing rate of heat evolution in the liquid due to a chemical reaction. If the chemical reaction is not too rapid the lags within the liquid should indeed be smaller than those indicated by the equation obtained below since for any short time interval during which the rate of heat evolution is approximately constant the initial temperature will not be uniform as assumed in the derivation.

The fundamental equation for this case is

$$\frac{1}{r}\frac{\partial}{\partial r}\left(r\frac{\partial T}{\partial r}\right)=\frac{c\rho}{k}\frac{\partial T}{\partial t}-\frac{Q}{k}, \quad 0\leq r\leq R,$$

and the boundary conditions are

$$2\pi kR\left(\frac{\partial T}{\partial r}\right)_{r=R}+K\left(\frac{\partial T}{\partial t}\right)_{r=R}+eT'=0$$

and

$$T(r, 0)=T_0.$$

The substitutions

$$T=T_0+\Theta(r, t)+\frac{Q}{c\rho}t, \quad x=\frac{r}{R},$$

reduce this problem to the boundary value problem discussed above. Introduction of the appropriate quantities gives the result

$$\frac{T(r, t)-T_0}{Q'}=\frac{Qt}{c\rho Q'}-\frac{1}{\pi k(1+2\lambda)}\times\left[\tau+\frac{\pi c\rho r^2\lambda}{2K}-\sum_{n=0}^{\infty}c_n e^{-\alpha_n^2\tau}J_0\left(\alpha_n\frac{r}{R}\right)\right], \quad (19)$$

where all the symbols have the same meaning as in Eq. (18), except that $Q'=KQ/c\rho+eT'$, Q being the rate of heat evolution per cubic centimeter in the liquid.

It is evident that the time lags will be practically independent of the rate of heat evolution as long as the quantity eT' is small compared with $KQ/c\rho$. Values of $\tau_{\min}$ could be calculated in the same manner as for Case I. For cases of interest in calorimetry where R will not be very different from unity and K will not be large the values of $\tau_{\min}$ given in Table II will hold here with fair accuracy.

In conclusion, the author wishes to express his thanks to Professor Lars Onsager for calling to his attention the method of treating the nonhomogeneous boundary value problem.

LETTERS TO THE EDITOR

This section will accept brief reports of new work of general interest to industrial physicists. The Editorial Board will not hold itself responsible for opinions expressed by the correspondents. Contributions to this section must reach the office of the Managing Editor not later than the twenty-fifth of the month preceding that of the issue in which the letter is to appear.

Some Observations on the Movement and Demagnetization of Ferromagnetic Particles in Alternating Magnetic Fields

In answer to Mr. H. S. Hatfield's discussion of the above subject on page 55 of your February issue, I would like to contribute additional observations to substantiate my previous contention that the movement of magnetized particles may be due to their reorientation in alternating magnetic fields and to reiterate the fact that demagnetization produced by *damped* H.F. alternating magnetic fields, as opposed to the condition resulting from ordinary alternating fields of frequencies of the order of 100 cycles, is a rather stable condition.

Mr. Hatfield's discussion indicates the desirability of making a distinction between particle movement along a horizontal supporting surface and the action that takes place when particles jump into the air above the surface. Mr. Hatfield's explanation suffices for the former movement but does not account adequately for the activity exhibited in the latter instance.

This jumping activity, in which I have been particularly interested, appears to be due to the reorientation tendency of magnetized particles. On slowly reversing the field by manually reversing the direction of direct current flowing through the windings of the solenoid of an electromagnet, magnetized particles resting on a horizontal surface above one pole become reoriented at each reversal, often turning end over end synchronously. At any given instant when the current is flowing, one end of a magnetized particle is attracted and the other repelled. Movement of the attracted end, when the supporting plane is above the magnet pole, is prevented by the surface, but the other end is free to lift up due to repulsion between the particle pole at this end and the like pole of the electromagnet. The reverse is true if the supporting surface is placed below a magnet pole.

As the frequency increases, the rate of rotation keeps pace for a time, and even at 100 cycles per second the tendency toward reorientation is certainly present and its effectiveness is related to the inertia of the particle and the frequency. This rotation permits the particle to attain a considerable kinetic energy so that each time it hits the surface the particle is thrown into the air again in a more or less random fashion, the direction taken depending upon the direction of particle rotation, the angle at which it strikes the surface, the nature of the surface, the shape of the particle, and other factors. Particles having a high coercive force, when placed in a properly regulated alternating field, often jump several centimeters away from their supporting surface.

Additional tests have been made on the use of damped high frequency magnetic fields for demagnetizing material of high coercive force. A more powerful magnet than that used previously was constructed by winding number 18 magnet wire around a fiber tube $1\frac{1}{4}$ inches outside diameter for a length of $4\frac{1}{2}$ inches to a total diameter of six inches. A knife switch surrounded by a 4-microfarad condenser served to break the current. This coil draws 6 amperes when connected to a 110-volt d.c. line. The oscillatory discharge produced by one sharp break of the circuit sufficed to demagnetize "Alnico," reported to have a coercive force in excess of 400 oersteds, in pieces $\frac{1}{2}$ inch in diameter and 3 inches long. Samples of cobalt magnet steel demagnetized in this way have remained demagnetized for a period of nine months.

C. W. DAVIS

Metallurgical Division,
U. S. Bureau of Mines,
Washington, D. C.,
May 4, 1936.